Bull. Min. Res. Exp. (2019) 159: 29-62

Bulletin of the Mineral Research and Exploration

http://bulletin.mta.gov.tr

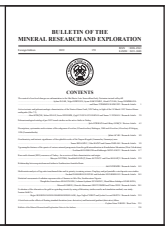

Active tectonic and paleoseismologic characteristics of the Yenice-Gönen fault, NW Turkey, in light of the 18 March 1953 Yenice-Gönen Earthquake (Ms=7.2)

Akın KÜRÇER[a*], Selim ÖZALP[b], Ersin ÖZDEMİR[c], Çağıl UYGUN GÜLDOĞAN[d] and Tamer Y. DUMAN[e]

[a]*General Directorate of Mineral Research and Exploration, Directorate of Geological Studies Department, 06800, Çankaya, Ankara, Turkey orcid.org/ 0000-0001-8646-5113*

[b]*General Directorate of Mineral Research and Exploration, Directorate of Geological Studies Department, 06800, Çankaya, Ankara, Turkey. orcid.org/0000-0002-6755-4206*

[c]*General Directorate of Mineral Research and Exploration, Directorate of Geological Studies Department, 06800, Çankaya, Ankara, Turkey orcid.org/0000-0002-8987-8842*

[d]*General Directorate of Mineral Research and Exploration, Energy Raw Materials Survey and Exploration Department, 06800, Çankaya, Ankara, Turkey orcid.org/ 0000-0002-1039-6542*

[e]*Fugro Sial Geoscience Consulting and Engineering Limited Company, Ankara, Turkey orcid.org/ 0000-0003-3556-2217*

Research Article

Keywords:
1953 Yenice-Gönen earthquake, Yenice-Gönen fault, North Anatolian Fault System, Slip rate, Paleoseismology

ABSTRACT

The Yenice-Gönen Fault (YGF) is located in the central part of the Biga Peninsula between Gönen and Yenice and is a right-lateral strike-slip active fault with general trending N65°E. On 18 March 1953 there was an earthquake on the YGF that died 263 people (Ms=7.2) and a 70 km surface rupture developed during this earthquake. In this study measurements of slip distribution were performed on the surface rupture of the Yenice-Gönen Earthquake (YGE) and the annual slip rate on the YGF was calculated. Right-lateral displacements of between 1.70±0.1 and 3.20±0.2 metres were measured on the surface rupture of the YGE. The maximum displacements were in an area close to the central part of the YGF (between Çakır and Karaköy village) and these values decreased relatively in NE and SW directions, documenting that was the bilaterally surface rupture propogation during the YGE. In the last 300.000 years, a total offset of 800±50 metres was measured on Gönen River and annual slip rate of 2.65±0.15 mm was calculated along the YGF. Current GPS studies show right-lateral strike-slip faults in the South Marmara region have slip rates of 6-8 mm/year. This slip rate is assessed as being partitioned between the YGF, Sarıköy Fault and Çan-Biga Fault zones which represent extensions of the North Anatolian Fault system within the South Marmara region. Paleoseismology studies determined that in the last 6200 years 6 earthquakes resulting in surface ruptures have occurred on the YGF, including the 1953 earthquake. According to the ^{14}C and OSL dating results, the variable and irregular earthquake recurrence interval of YGF is ranging from 505 to 1793 years. In this study average earthquake recurrence interval of YGF was determined as 1180 years.

Received Date: 30.01.2018
Accepted Date: 14.05.2018

1. Introduction

As a result of progressive deformation developing linked to continental collision between the African, Arabian and Eurasian plates in the Eastern Mediterranean Region, four main neotectonic regions have developed separated by the North Anatolian Fault system (NAFS), East Anatolian Fault system (EAFS), Dead Sea Fault Zone (DSFZ) and the active subduction zone of the Aegean-Cyprus arc (McKenzie, 1972, 1978; Şengör, 1979, 1980; Jackson and McKenzie, 1984; Şengör et al., 1985; Taymaz et

Citation Info: Kürçer, A., Özalp, S., Özdemir, E., Uygun Güldoğan, Ç., Duman, T. Y. 2019. Active tectonic and paleoseismologic characteristics of the Yenice-Gönen Fault, NW Turkey, in light of the 18 March 1953 Yenice-Gönen Earthquake (Ms=7.2). Bulletin of Mineral Research and Exploration, 159, 29-62. *http://dx.doi.org/10.19111/bulletinofmre.500553*

** Corresponding author: Akın KÜRÇER, akin.kurcer@mta.gov.tr*

al., 1991; LePichon et al., 1995; Armijo et al., 1999; Bozkurt, 2001). Currently, NW Turkey, is deformed by the western extensions of the NAFS (Figure 1).

The North Anatolian Fault system (NAFS) is a right-lateral strike-slip active fault system with nearly 1500 km length characterised by large earthquakes produced in the last century (Figure 1; Barka and Kadinsky-Cade, 1988). One of the most active fault systems in the Eastern Mediterranean Region in terms of seismicity, the NAFS begins at the Karlıova triple junction and extends in a linear zone to nearly 100 km east of Adapazarı. The NAFS divides into a northern and southern branch in this region due to the effect of variable stress states and forms a large-scale horsetail structure (Barka and Gülen, 1988; Şengör and Barka, 1992) (Figure 1). From east of Adapazarı the northern branch of the NAFS extends within Lake Sapanca to the Sea of Marmara. Within the Sea of Marmara, the system is represented by the Adalar, Avcılar, Kumburgaz and Tekirdağ segments from east to west, respectively (Emre et al., 2013). The northern branch extends nearly W-E through the Sea of Marmara, before bending toward the SE near Şarköy to enter the Gulf of Saros and the North Aegean Sea (Figure 2).

The southern branch extending with nearly E-W trending in Dokurcun Valley and south of the Sea of Marmara, is represented by the Geyve, İznik-Mekece and Gemlik Faults in this area from east to west, respectively. Between the Bay of Gemlik and Kapıdağ Peninsula, along the south coast of the Sea of Marmara, the southern branch makes a restraining bend to the SW from Kapıdağ Peninsula to extend into the Biga Peninsula. The southern branch of the NAFS extends from the NE of the Biga Peninsula to the SW and is represented by the Edincik, Sinekçi, Çan-Biga fault zone, Sarıköy, Bekten, Yenice-Gönen, Evciler faults and Edremit fault zone (Figure 2).

Destructive earthquakes have occurred in the historical and instrumental periods on the western part of the NAFS (Tables 1 and 2) (Figure 2). The YGF, one of the most active fault segments of the NAFS in south of Marmara produced an Ms=7.2 magnitude earthquake on 18 March 1953 and this earthquake

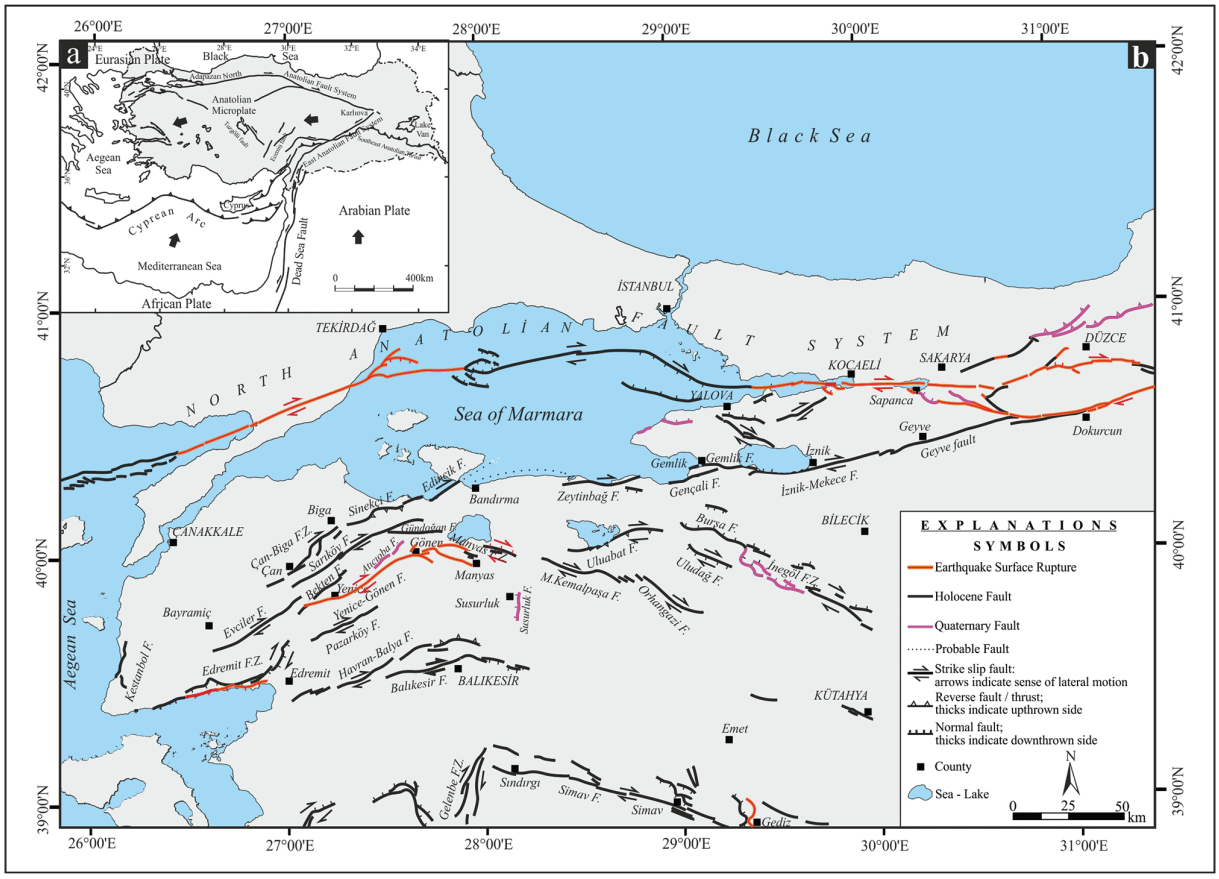

Figure 1- Simplified active fault map of northwest Anatolia (Emre et al., 2012).

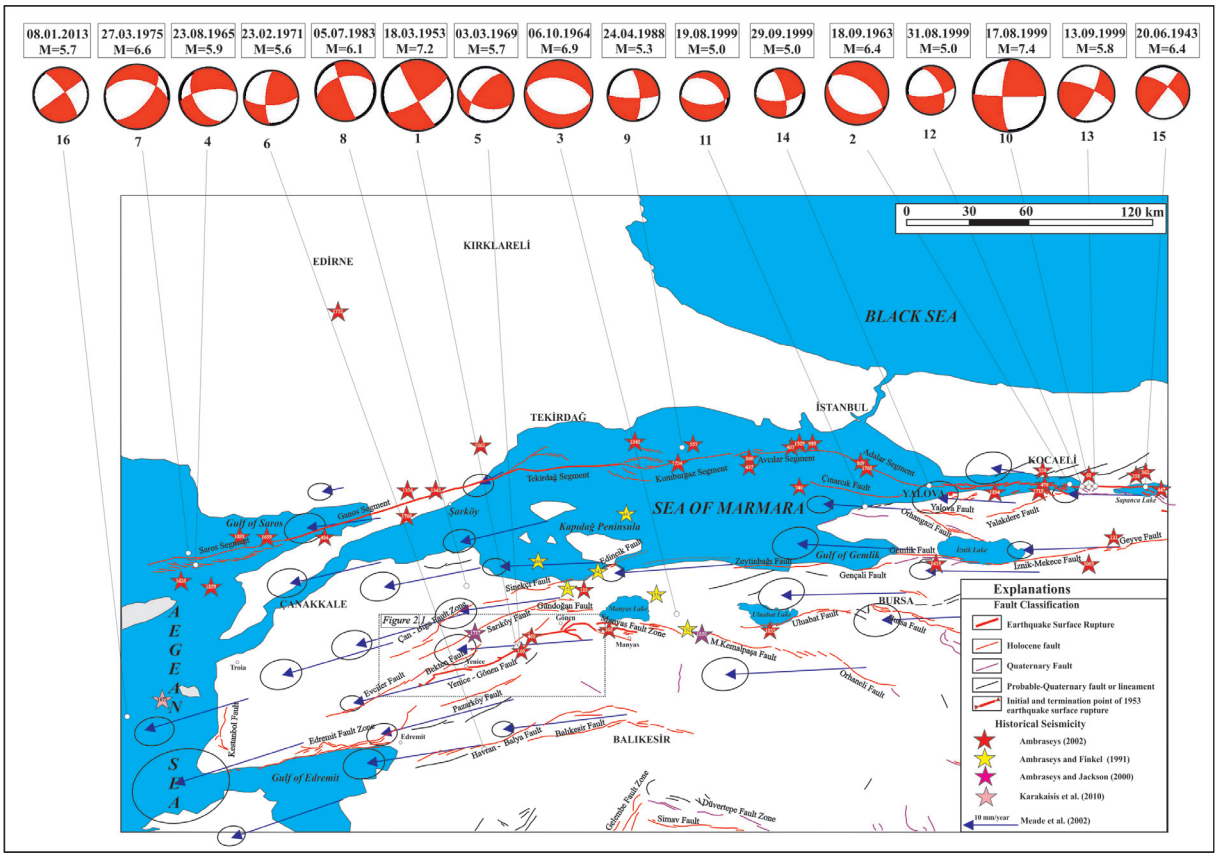

Figure 2- Active and capable active faults were drawn from Emre et al (2013) and in their references. GPS vectors taken from Meade et al. (2002). For historical and instrumental period earthquakes and focal mechanism solution references please see tables 1 and 2.

caused a surface rupture with nearly 70 km length between the east of Gönen and the southwest of Yenice (Kürçer, 2006; Kürçer et al., 2008) (Figure 2).

After the 18 March 1953 YGE the first macroseismic observations were made by Ketin and Roesly (1953), who recorded right lateral displacements varying from 4,3 m to 1,5 m along the surface rupture with total length of 50 km. Ketin and Roesly (1953) proposed the rupture progressed from E to W during the earthquake considering the P and S wave motion times. Another macroseismic study related to the YGE was completed by Pınar (1953). According to Pınar (1953), the YGE occurred on the southern branch of the NAFS and created a surface rupture with total 60 km length between the Sea of Marmara and the Gulf of Edremit. Focal mechanism solutions indicating the YGE was caused by a NE-SW striking right lateral strike-slip fault were made by McKenzie (1972). According to Herece (1990), the length of the surface rupture developing during the YGE was 50 km. The researcher stated the YGF experienced several faulting periods in the Quaternary based on fault scarps at different erosion levels observed during surface rupture mapping. Herece (1990) proposed that the total right lateral offset of the YGF was 2,8 km from the Late Pliocene to the present and annual slip rate was 1,4 mm. A study of active tectonism in central and northern Aegean by Taymaz et al. (1991) stated the thrust component was dominant during the 1969 Gönen earthquake (see figure 2) and indicated that the Biga Peninsula was rising due to this compression.

GPS studies in the Marmara region (Straub, 1996; Straub and Kahle, 1997; Reilinger et al., 1997; Meade et al., 2002; Kreemer et al., 2004; Reilinger et al., 2006) reveal the annual right lateral movement of the Anatolian block relative to Eurasia is 20-25 mm and this is mainly distributed along the NAFS. Straub (1996) proposed that the majority of this movement was on the northern branch of the NAFS with the remaining portion distributed along the southern branch. Meade et al. (2002) proposed annual slip rates from right-lateral strike-slip faults and normal faults which were extensions of the NAFS in the Marmara region based on GPS measurements. Accordingly, the

Table 1- Large historical earthquakes occurring in northwest Turkey.

Date	Degree of latitude (N)	Degree of longitude (E)	Magnitude (M)	Location	Reference
32	40,5	30,5	7,0	Nicaea (İznik)	Ambraseys (2002)
68	40,7	30,0	7,2	Nicaea (İznik)	Ambraseys (2002)
121	40,5	30,1	7,4	Nicomedia (İzmit)	Ambraseys (2002)
10.11.123	40,3	27,7	7,0	Cyzicus (Erdek)	Ambraseys (2002)
155				Hellespont and Bithynia	Ambraseys and Finkel (1991)
160	40,0	27,5	7,1	Hellespont (Ç. straits)	Ambraseys (2002)
03.05.180	40,6	30,6	7,3	Nicomedia (İzmit)	Ambraseys (2002)
268	40,7	29,9	7,3	Nicomedia (İzmit)	Ambraseys (2002)
24.08.358	40,7	30,2	7,4	İzmit	Ambraseys (2002)
02.12.362	40,7	30,2	6,8	İzmit	Ambraseys (2002)
11.10.368	40,5	30,5	6,8	Persis	Ambraseys (2002)
368	40,1	27,8	6,8	Germe	Ambraseys (2002)
01.04.407	40,9	28,7	6,8	Hebdomon (Bakırköy)	Ambraseys (2002)
25.09.437	40,8	28,5	6,8	İstanbul	Ambraseys (2002)
06.11.447	40,7	30,3	7,2	Nicomedia (İzmit)	Ambraseys (2002)
07.04.460				Cyzicus (Erdek)	Ambraseys and Finkel (1991)
25.09.478	40,7	29,8	7,3	Helenopolis	Ambraseys (2002)
484	40,5	26,6	7,2	Callipolis	Ambraseys (2002)
06.09.543				Cyzicus (Erdek)	Ambraseys and Finkel (1991)
16.08.554	40,7	29,8	6,9	Nicomedia (İzmit)	Ambraseys (2002)
14.12.557	40,9	28,3	6,9	Silivri	Ambraseys (2002)
26.10.740	40,7	28,7	7,1	Marmara	Ambraseys (2002)
23.05.860	40,8	28,5	6,8	Marmara	Ambraseys (2002)
09.01.869	40,8	29,0	7,0	CP	Ambraseys (2002)
02.09.967	40,7	31,5	7,2	Bolu	Ambraseys (2002)
25.10.989	40,8	28,7	7,2	Marmara	Ambraseys (2002)
23.09.1063	40,8	27,4	7,4	Panio	Ambraseys (2002)
1065	40,4	30,0	6,8	Nicaea (İznik)	Ambraseys (2002)
01.06.1296	40,5	30,5	7,0	Bithynia	Ambraseys (2002)
1323				İstanbul	Ambraseys and Finkel (1991)
18.10.1343	40,7	27,1	6,9	Ganos	Ambraseys (2002)
18.10.1343	40,9	28,0	7,0	Heraclea	Ambraseys (2002)
01.03.1354	40,7	27,0	7,4	Hexamili	Ambraseys (2002)
15.03.1419	40,4	29,3	7,2	Bursa	Ambraseys (2002)
10.09.1509	40,9	28,7	7,2	CP	Ambraseys (2002)
10.05.1556				Sea of Marmara	Ambraseys and Finkel (1991)
18.05.1625	40,3	26,0	7,1	Saros	Ambraseys (2002)
17.02.1659	40,5	26,4	7,2	Saros	Ambraseys (2002)
14.02.1672	39,7	25,8	7,0	Bozcaada	Karakaisis et al. (2010)
25.05.1719	40,7	29,8	7,4	İzmit	Ambraseys (2002)
06.03.1737	40,1	27,3	7,0	Aşağı İnova	Ambraseys and Jackson (2000)
29.07.1752	41,5	26,7	6,8	Edirne	Ambraseys (2002)
02.09.1754	40,8	29,2	6,8	İzmit	Ambraseys (2002)
22.05.1766	40,8	29,0	7,1	Marmara	Ambraseys (2002)
05.08.1766	40,6	27,0	7,4	Ganos	Ambraseys (2002)
19.04.1850	40,1	28,3	6,1	Between Lakes Manyas and Uluabat	Ambraseys and Jackson (2000)
28.02.1855	40,1	28,6	7,1	Bursa	Ambraseys (2002)
21.08.1859	40,3	26,1	6,8	Saros	Ambraseys (2002)
09.02.1893	40,5	26,2	6,9	Saros	Ambraseys (2002)

Table 2- Fault plane solutions for the instrumental period earthquakes listed in figure 2 (adapted from Şengör et al., 2004).

No	Date (day. month. year)	Time (hour: minute) GMT	Degree of latitude (N)	Degree of longitude (E)	Magnitude	Depth (km)	Strike (°)	Dip (°)	Rake (°)	Reference
1	20.06.1943	15:33	40,83	30,48	6,4	?	176	76	0	McKenzie (1972)
2	18.03.1953	19:06	40,01	27,49	7,2	10*	59	84	14	McKenzie (1972), Ayhan et al. (1981)
3	26.05.1957	06:33	40,58	31,00	7,0	?	87	78	179	McKenzie (1972)
4	26.05.1957	09:36	40,80	30,80	6,0	?	114	24	-166	Canıtez and Üçer (1967)
5	27.05.1957	11:01	40,70	31,00	5,5	?	293	74	157	Canıtez and Üçer (1967)
6	18.09.1963	16:58	40,71	29,09	6,4	15	304	56	-82	Taymaz et al. (1991)
7	06.10.1964	14:31	40,20	28,20	6,9	14	100	40	-90	Taymaz et al. (1991)
8	23.08.1965	14:08	40,39	26,12	5,9	33	261	70	-132	Kocaefe and Ataman (1976)
9	22.07.1967	16:56	40,67	30,69	7,1	12	275	88	-178	Taymaz et al. (1991)
10	30.07.1967	01:32	40,72	30,52	5,6	16	301	50	70	McKenzie (1972)
11	03.03.1969	00:59	40,08	27,50	5,7	4	219	65	45	McKenzie (1972)
12	23.02.1971	19:41	39,62	27,32	5,6	10	86	66	160	Papadopoulos et al. (1986)
13	27.03.1975	05:15	40,45	26,12	6,6	15	279	46	-43	Jackson and McKenzie (1984)
14	05.07.1983	23:02	40,33	27,21	6,1	15	254	49	-173	Harvard Univ. (1998)
15	24.04.1988	20:49	40,88	28,24	5,3	15	356	71	-11	Harvard Univ. (1998)
16	17.08.1999	00:01	40,70	29,99	7,4	9	91	87	164	GCMT Catalogue
17	17.08.1999	03:14	40,59	30,62	5,3	8	192	32	-82	Örgülü and Aktar (2001)
18	19.08.1999	15:17	40,65	29,09	5,0	4	92	60	-110	Örgülü and Aktar (2001)
19	31.08.1999	08:10	40,74	29,99	5,0	8.6	80	70	-143	Özalaybey et al. (2002)
20	13.09.1999	11:55	40,76	30,07	5,8	12	293	73	164	Örgülü and Aktar (2001)
21	29.09.1999	00:13	40,71	29,30	5,0	8	85	63	-161	Örgülü and Aktar (2001)
22	11.11.1999	14:41	40,78	30,29	5,5	20	307	66	179	Örgülü and Aktar (2001)
23	08.01.2013	14:16	39,65	25,50	5,7	8	54	89	-166	Kürçer et al. (2015)

right-lateral slip rate along the Uluabat and Manyas faults in the southern Marmara region was 3,6±2,0 mm with vertical offset rate of 8,0±3,4 mm; while along the YGF and Sarıköy İnova fault the annual right lateral offset was 6,8±2,3 mm and vertical slip rate was 0,8±3,4 mm. Another GPS study of active faults in the southern Marmara region by Kremmer et al. (2004) calculated the right-lateral strike-slip annual slip rate was 7 mm along the southern branch of the NAFS defined as the Bursa-Yenice-Gönen line. The approximately 7 mm/year right-lateral slip rate calculated by Meade et al. (2002) and Kremmer et al. (2004) for all faults belonging to the southern branch of the NAFS must be shared between different faults led by the Yenice Gönen and Sarıköy faults (Kürçer, 2008).

The first studies researching the paleoseismologic properties of the YGF were completed by Kürçer (2006) and Kürçer et al. (2008). Kürçer et al. (2008) dated three earthquakes on the YGF causing surface ruptures in the last 1400 years including the 1953 earthquake. The first of these earthquakes was in 620 AD and the second was in 1440 AD. Based on this age data, they proposed the average earthquake recurrence interval for the YGF was 660±160 years. Using the earthquake recurrence interval and a displacement amount of 4,2 metres, the researchers calculated the annual slip rate for the YGF as 6.3 mm and noted the compliance of this value with results obtained from GPS measurements. Dirik et al. (2008) in a study researching the neotectonic and paleoseismologic properties of the YGF reported the surface rupture length of the YGF was 60 km. The researchers measured 65 to 495 cm right lateral displacement during the YGE. Cumulative displacement amounts measured along the YGF varied from 6,8 to 38 m. Based on the cumulative offset values on the Seyvan,

Karasu and Gönen segments, Dirik et al. (2008) proposed at least five earthquakes had occurred. A study of the seismotectonics of the Biga Peninsula and south Sea of Marmara by Özden et al. (2008) revealed that the faults located in the north of the Biga Peninsula were currently transpressive while the faults located in the south were mainly transtensive in character. On the Revised Turkish Active Fault map, Emre et al. (2013) assessed the YGF as a 67 km long, active fault comprising 4 geometric segments. The researchers adapted the 5 km value recommended by Duru et al. (2012) in the Hallaçlar formation near Yenice as the total offset on the YGF. Based on GPS studies (Meade et al., 2002; Kremmer et al., 2004), Emre et al. (2013) proposed that the recommended 6-8 mm total annual slip rate proposed for all the NE-SW oriented faults in the Biga Peninsula was equally shared between the YGF, Sarıköy Fault and Biga-Çan fault zone. From this aspect, they proposed the annual slip rate on the YGF was 2-3 mm. A study researching historical earthquakes affecting ancient city of Troy by Kürçer et al. (2012) proposed that Troy III (2200-2050 BC) and Troy VI (1800-1275 BC) settlements were destroyed by earthquakes and that these earthquakes may be due to active faults in the area. According to izoseist maps of the 1912 Şarköy-Mürefte (Mw=7.2), 1953 Yenice-Gönen (Mw=7.2) and 1983 Biga (Mw=6.8) earthquakes occurring near Troy in the last century, the researchers stated these earthquakes affected the Troy region with VIII-X intensity (MSK). Based on this they noted that active faults in the Biga Peninsula may have affected the Troy region in the historical period. The researchers recommended that earthquake dates obtained from paleoseismological studies to be completed in the Biga Peninsula should be compared with the destruction times of Troy III and VI settlements.

In this study, comprehensive active fault and paleoseismology studies completed on the surface rupture of the 18 March 1953 Yenice-Gönen earthquake were used to research the active tectonic and paleoseismologic properties of the YGF and re-evaluate it within the regional tectonic framework.

2. Geology of Yenice-Gönen Fault and Surroundings

In the study area, there are outcrops of different age from the Palaeozoic to the present and types of rock units (Figure 3). Pre-Tertiary aged rocks in the Biga Peninsula and surroundings are composed of four tectonic belts with trending NE-SW (Duru et al., 2012). These are the İzmir-Ankara Zone / Bornova Flysch, Sakarya Zone, Çetmi Melange and Ezine Zone, from east to west, respectively.

The basement units near the YGF and surroundings located in the central part of the Biga Peninsula comprises the Kazdağ Metamorphics belonging to the Sakarya zone. In the study area the Kazdağ Metamorphics are represented by the Sütüven formation (Cs).

These units are overlain by the metamorphics of the Late Paleozoic age Kalabak Group with a tectonic contact. Comprising low-grade metamorphics, the Kalabak Group Metamorphics are represented by the Torasan formation (Pzt) comprising marble and phyllite and schists with metaserpentinite lenses at the base and the Sazak formation (Pzs) comprising metatuffs with marble intercalations at the top (Duru et al., 2012).

The Torasan metamorphics in the Kalabak Group are cut by the Çamlık Metagranodiorite (Pzç) consisted of metagranodiorite and granitic gneiss (Duru et al., 2012).

The Kalabak Group Metamorphics are tectonically overlain by Karakaya Complex (Okay and Göncüoğlu, 2004; Aysal et al., 2012*a,b*). The Karakaya Complex comprises Late Permian (?)-Triassic aged units with mainly tectonic contacts but occasional transitions. Within the Karakaya Complex, undifferentiated units of metaconglomerate, metasandstone, sandy limestone, tuff, metavolcanics and Devonian, Carboniferous and Permian-aged limestone blocks are defined as Karakaya Complex units (Trkk) (Duru et al., 2012). Additionally, the Karakaya Complex is represented by arkosic sandstone (Trka), Mehmetalan formation (Trkm) and Çal formation (Trkç) from bottom to top.

The Karakaya Complex units are unconformably overlain by the Lias-aged Bayırköy formation comprising continental and shallow marine conglomerates, sandstone, mudstone and limestone.

Toward the top of the Bayırköy formation, there is a transition to the Callovian-Hauterivian-aged Bilecik formation comprising platform-type limestones. Above the Bilecik formation, there is a conformable transition to the hemipelagic, micritic limestone and claystone alternations of the Hauterivian-Albian-aged

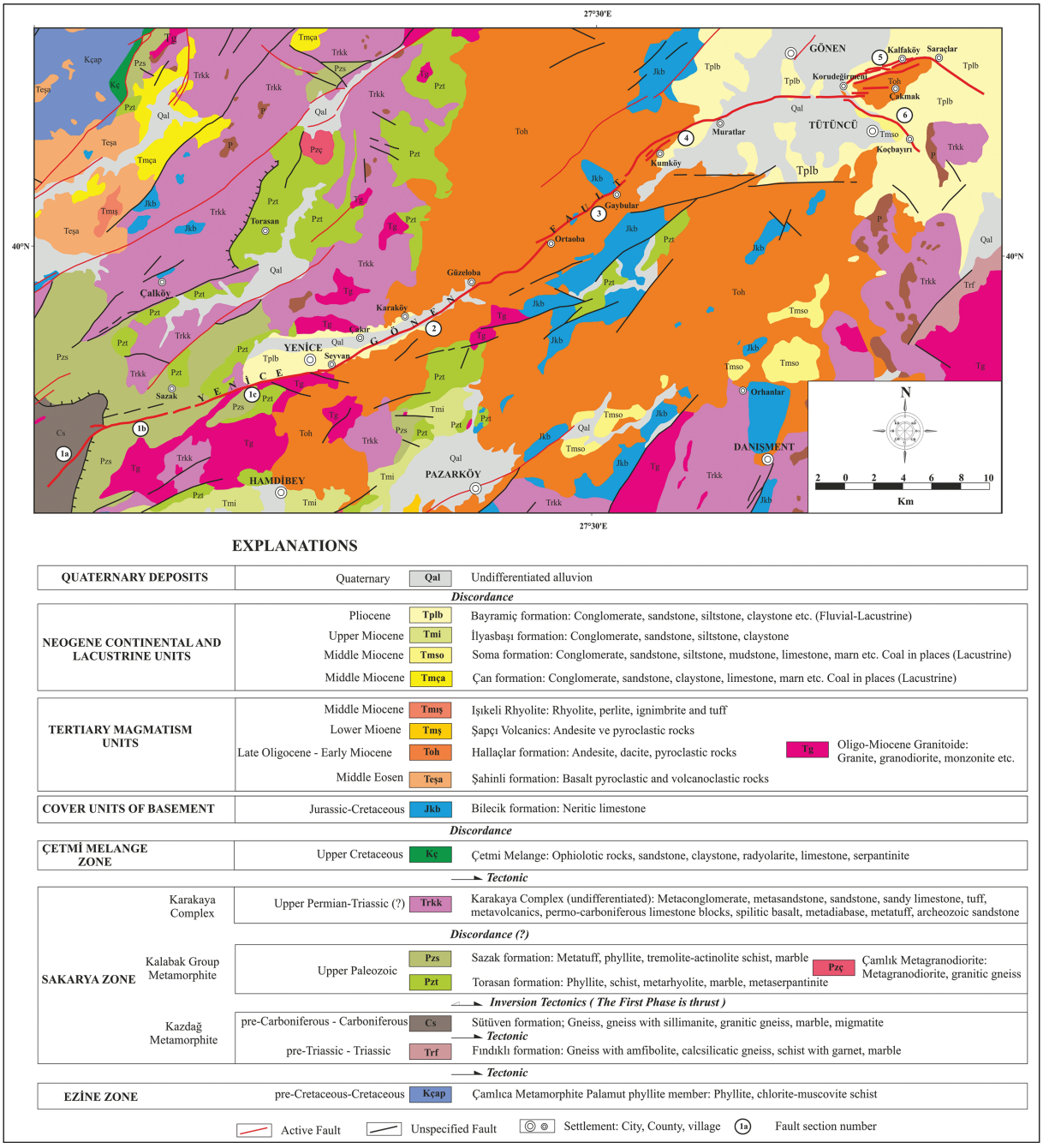

Figure 3- Geologic map of the central part of the Biga Peninsula (adapted from Duru et al., 2012).

Pınar formation (Duru et al., 2012). These cover units above basement units are only represented within the study area by the Bilecik formation with very limited outcrop area NE of Yenice.

The study area contains, volcanic units of Tertiary magmatism, volcanosedimentary sequences and granitoids (Altunkaynak et al., 2012; Aysal, 2015). Products of Tertiary magmatism outcrop in larger areas of the central part of the Biga Peninsula and are represented by the Middle Eocene Şahinli formation, Late Oligocene-Early Miocene Hallaçlar formation and the coeval Tertiary granitoids, Lower Miocene Şapçı Volcanics and Middle Miocene Işıkeli Rhyolite (Karacık et al., 2008; Aysal et al., 2012*b*). In the Biga Peninsula, mainly closed basins developed under control of active faults with terrestrial sediments and/or lacustrine carbonate rocks deposited in fluvial or

lake environments. These units comprise Middle Miocene sediments and coals of the Çan and Soma formations, Upper Miocene sediments of the İlyasbaşı formation and Pliocene sediments and occasional carbonates of the Bayramiç formation. Quaternary-Holocene modern sediments unconformably cover all these units.

3. Segment Structure of Yenice-Gönen Fault

The YGF is an active fault that has produced more than one earthquake resulting in surface rupture in the geologic past. In the literature, "earthquake segments" are defined as differentiable sections of an active fault producing earthquakes with two or more surface ruptures (dePolo et al., 1989, 1991). Therefore, the YGF is assessed as an earthquake segment with proven seismicity based on the 1953 earthquake and paleo-earthquakes identified in this study. Within fault segments, shorter sections separated from each other by step or bend structures are assessed as fault sections.

The YGF comprises 6 fault sections with lengths varying from 5,5 to 19 km separated by restraining or releasing bends or steps. These are named the Sazak, Çakır, Gaybular, Muratlar, Kalfaköy and Tütüncü fault sections from SW to NE (Figures 3 and 4).

The Sazak section has total length of 19 km and comprises three sub-sections separated by en-echelon offset-overlapping steps (Figure 3). The section in the SW has N45°E strike and 6 km length (1a on Figure 3). This section of the fault extending from Sakardağı to Sazak Stream is observed within the Sütüven formation (Cs) belonging to the Kazdağ Metamorphics. The second subsection of the Sazak section is 6,5 km long and begins in the west at Kale Hill and is observed to continue west of Sazak Valley with N75°E strike (1b on Figure 3). In this section the fault cuts a normal fault contact between the Sütüven formation (Cs) belonging to the Kazdağ Metamorphics and the Sazak formation (Pzs) belonging to the Kalabak Group, offsetting it to the right-laterally. The easternmost part of the Sazak section is 9,5 km long (1c on Figure 3). The fault in this section extends with N85°E strike between Sazak Valley and Yenice and forms the boundary between the Sazak formation (Pzs) and Quaternary-aged alluvial sediments in the Sazak Valley. From east of Sazak Valley to Yenice, it controls the contacts between the Sazak formation (Pzs) with the Torasan formation (Pzt) of the Kalabak Group, between Tertiary granitoids (Tg) and Karakaya Complex units (Trkk) and between Tertiary granitoids and Plio-Quaternary basin sediments of the Yenice Basin (Tplb) (Figure 3).

The Sazak section is separated from the Çakır section by a 200 m wide and 500 m long restraining step in the south of Yenice. The Çakır section has total length of 19 km between Yenice and Ortaoba (2 on Figure 3). With E-W strike between Yenice and Seyvan, the fault bends to the left SW of Seyvan Village to extend towards the east of Çakır with

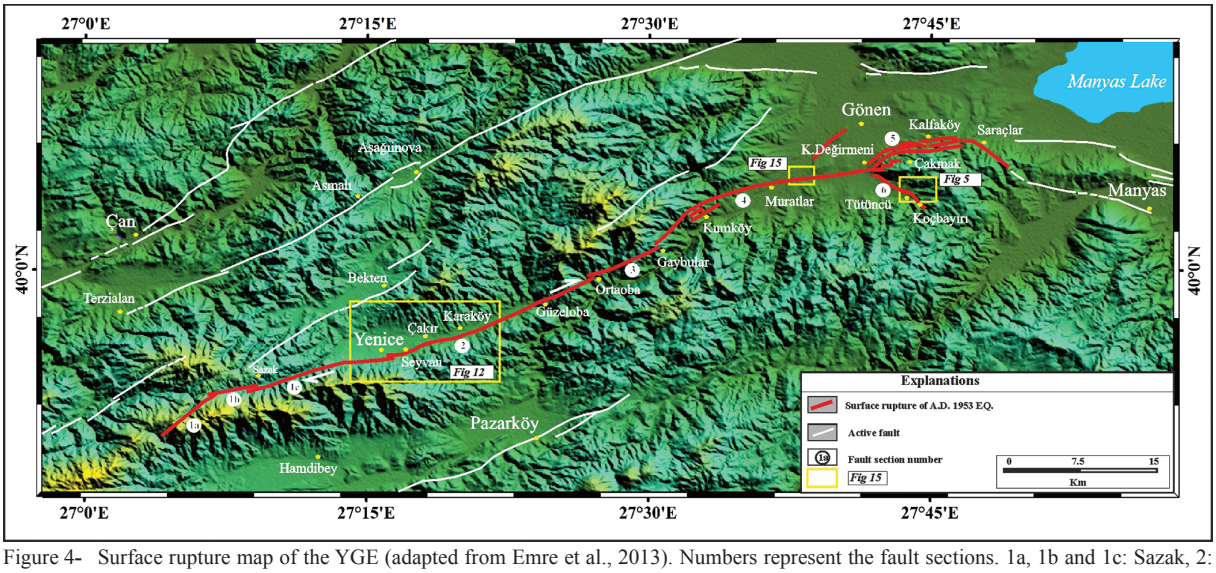

Figure 4- Surface rupture map of the YGE (adapted from Emre et al., 2013). Numbers represent the fault sections. 1a, 1b and 1c: Sazak, 2: Çakır, 3: Gaybular, 4: Muratlar, 5: Kalfaköy, 6: Tütüncü..

N67°E general trending. In this section the fault has reverse component the effect of restraining bending. East of Çakır the fault again bends toward the left and extends to the west of Güzeloba with N67°E strike. The remaining easternmost part of the Çakır section between Güzeloba and Ortaoba villages is characterised by bends to the right and left. The Çakır section cuts Tertiary granitoids and the Late Oligocene-Early Miocene Hallaçlar formation between Yenice and Seyvan. South of Seyvan, the fault controls the contact between the Hallaçlar formation and Yenice basin sediments and occasionally cuts Late Quaternary-Holocene alluvial sediments in this area. Between Çakır and Karaköy, the fault mainly cuts Yenice (Small Agonia) stream sediments entering the Hallaçlar formation east of Karaköy and is observed within these units until the east boundary of the fault section.

NW of Ortaoba, a 750 m long, 250 m wide left step separates the Çakır section from the Gaybular section with 10 km length (3 on Figure 3). Extending from southwest of Kumköy to Çatalçal hill with N55°E trending, the Gaybular section is mainly observed within the Hallaçlar formation, occasionally cutting neritic limestones belonging to the Jurassic-Cretaceous Bilecik formation.

The Gaybular section is separated from the Muratlar section by a 3 km long, 500 m wide restraining bend west of Kumköy (4 on Figure 3). The Muratlar section has total length of 16 km and extends with N65°E trending between Kumköy and Gönen Stream before bending toward the right from Gönen Stream to extend west of Çakmak Village with E-W trending. The Muratlar section brings the Hallaçlar formation side-by-side with Pliocene clastic sediments of the Bayramiç formation between Kumköy and Muratlar. East of Muratlar, the fault cuts alluvial sediments of Gönen Stream, before cutting sediments from the Bayramiç formation south of Korudeğirmeni and ending within the Hallaçlar formation.

Comprising the easternmost section of the main body of the YGF, the Kalfaköy section extends with general trend of N60°E from west of Korudeğirmeni to east of Saraçlar village (5 on Figure 3). With total length of 6 km, the section is represented by a 300 m wide deformation zone. The Kalfaköy section ends with a bend to the SE (Saraçlar bend) near Saraçlar village. This section is also to the section where the Yenice-Gönen Fault overlaps with the surface rupture of the 1964 Manyas earthquake. The majority of the Kalfaköy section controls the contact between the Hallaçlar formation and the Bayramiç formation.

The 5,5 km section of the YGF between Korudeğirmeni and Koçbayırı villages with N70°W trending is named the Tütüncü section (6 on Figure 3). The Tütüncü section is a splay fault of the YGF extending toward the SE. The fault gains a reverse component making a bend to the left north of Tütüncü (Figure 5). The majority of the Tütüncü section controls the contact between the Bayramiç formation and the Soma formation, occasionally cutting the Soma formation and alluvial fan sediments.

4. 18 March 1953 Yenice-Gönen Earthquake (Ms=7.2) Surface Rupture

On 18 March 1953 at 19:06 (GMT) in southern Marmara (Coordinates: 40.01 N – 27.49 E), an earthquake (Ms=7.2) occurred with 10 km focal depth (Ayhan et al., 1981). As a result of the earthquake, 263 people died, more than 8000 buildings were damaged, 211 schools, 176 official buildings and 27 mosques were destroyed (Barka et al., 2002). The earthquake was felt in Çanakkale, Edirne, İstanbul, Adapazarı, Bursa, Balıkesir, Dikili, Foça and Karaburun. According to focal mechanism solutions, the source of earthquake is a N59°E trending right-lateral strike-slip fault (Canıtez and Üçer, 1967; McKenzie, 1972). A total surface rupture length of 70 km was caused by the YGE (see figures 3 and 4). In this study, observations of the 1953 YGE surface rupture were made at a total of 28 points (Table 3).

The first point where the 1953 YGE surface rupture traces can be observed is Dede Çeşme near Taşlıburun Ridge southwest of Yenice (YGF-01 in Table 3). At this location the YGE offsets a stream by 1,70±10 cm right-laterally and 50±5 cm vertically.

South of Yenice a 200 m wide and 500 m bend toward the left divides the Sazak section from the Çakır section, with total length of 19 km between Yenice and Ortaoba. Following E-W strike between ancient Yenice and Seyvan, the surface rupture bends 15° to the left from southwest of Seyvan Village with N75°E strike east of Çakır. In this area, the fault has reverse component due to the effect of restraining bends. This characteristic is clearly observed in trenches ezcavated south of Seyvan. The 1953 surface rupture is characterised by linear fault scarps between ancient

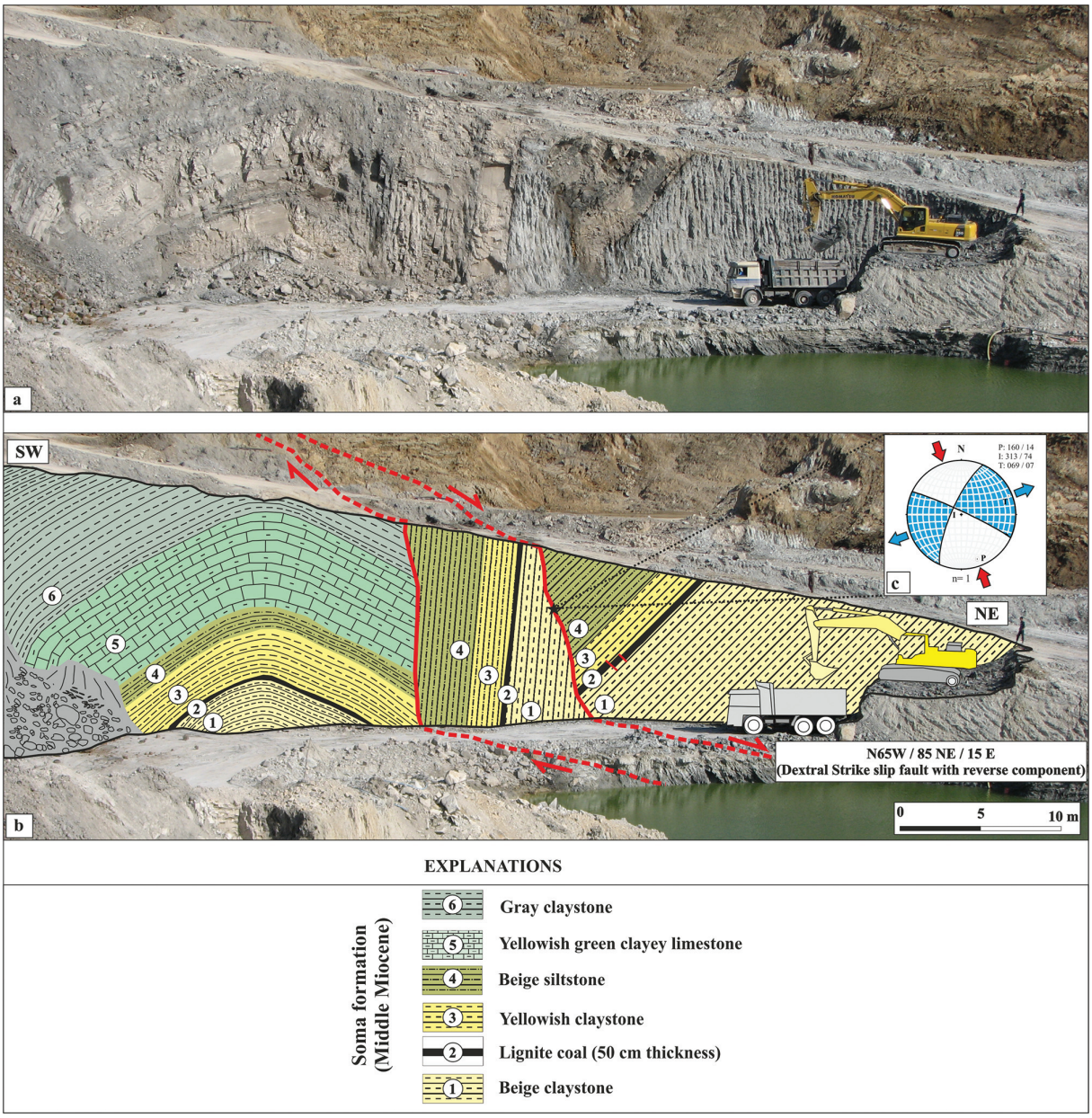

Figure 5- Structural properties of the Tütüncü fault section north of Tütüncü Village, a) Field photograph, b) Geological cross-section, c) Fault plane solution on Schmidt network hemisphere using Faultkin program (Almendinger et al., 2012).

Yenice and Seyvan (Figure 6). South of Seyvan, the fault forms the contact between the Late Oligocene-Early Miocene Hallaçlar formation and the Pliocene Bayramiç formation, cutting occasional alluvial fan sediments and slope debris. From east of Seyvan, the fault enters the Bayramiç formation and reaches south of Çakır by cutting the Yenice – Pazarköy road (Figure 7) N75°E (YGF-03 in Table 3).

The surface rupture of the 1953 earthquake extends with N70°E strike between Karaköy and Güzeloba. The easternmost part of the Çakır section between Güzeloba and Ortaoba villages is characterised by bends to the right and left. In this section the surface rupture is observed within the Late Oligocene-Early Miocene Hallaçlar formation. The surface rupture is observed as a crushed-brecciated fault zone in a stabilised road cut at the Kuştepe locale (YGF 17 in Table 3) located 1 km NE of Güzeloba village. According to information obtained from witnesses of the earthquake, there was a surface rupture southwest of Namazlık stream in Karasu (Karasuçam)

Table 3- Observation points of surface rupture of YGE (adapted from Kürçer, 2006).

Observation no	Sheet no	Coordinates (UTM)	Displacement amount (cm)	Explanation
YGF-01	İ 18 a2	35 0519481 E 44 18504 N	170±10 (right lateral) 50±5 (vertical)	Offset stream in Dede Çeşme locale west of Yenice
YGF-02	İ 18 b1	35 0525157 E 44 19713 N	2.86 (right lateral) 50±10 (vertical)	Linear fault scarps in trench area south of Seyvan
YGF-03	İ 18 b1	35 0527 125 E 44 21120 N	2.50 (right lateral)	Point where 1953 surface rupture cuts Yenice-Gönen road
YGF-04	İ 18 b1	35 0528759 E 44 21870 N	320±50 (right lateral)	South of Çakır, offset tree line west of the bridge
YGF-05	İ 18 b1	35 0528987 E 4421983 N	200±10 (right lateral)	South of Çakır, offset field boundary east of the bridge
YGF-06	İ 18 b1	35 0528786 E 4421884 N	190±30 (right lateral)	South of Çakır, offset field boundary west of the bridge
YGF-07	İ 18 b1	35 0528808 E 4421917 N	220±20 (right lateral)	South of Çakır, offset field boundary at west edge of the bridge
YGF-08	İ 18 b1	35 0529329 E 4421931 N	2200±200 (right lateral)	Cumulative stream offset SE of Çakır
YGF-09	İ 18 b1	35 0529655 E 4422068 N	2300±200 (right lateral)	Cumulative stream offset SE of Çakır
YGF-10	İ 18 b1	35 0528886 E 4421778 N	200±10 (right lateral)	Offset field boundary SE of Çakır
YGF-11	İ 18 b1	35 0529263 E 44 22035 N	320±20 (right lateral)	South of Çakır, offset field boundary east of the bridge
YGF-12	İ 18 b1	35 0529998 E 44 22325 N	300±30 (right lateral)	Offset field boundary SE of Çakır
YGF-13	İ 18 b1	35 0530015 E 44 22328 N	320±20 (right lateral)	Offset field boundary SE of Çakır
YGF-14	İ 18 b1	35 0530053 E 44 22358 N	310±20 (right lateral)	Offset field boundary SE of Çakır
YGF-15	İ 18 b2	35 0531779 E 4423208 N	1800±200 (right lateral)	Cumulative stream offset SE of Karaköy
YGF-16	İ 18 b2	35 0532046 E 44 23454 N	2100±200 (right lateral)	Cumulative stream offset SE of Karaköy
YGF-17	İ 18 b2	35 0536199 E 44 26017 N		Crush zone 1 km NE of Güzeloba
YGF-18	İ 18 b2	35 0538042 E 44 26787 N		N50°E-trending surface rupture 500 m SW of Karasukababaklar
YGF-19	İ 18 b2	35 0532046 E 44 23454 N		Reidel fracture in Karasubaklar Village
YGF-20	H 18 c3	35 0538883 E 44 28291 N		Earthquake surface rupture at Yolçatı locale 2 km north of Karasukababaklar
YGF-21	H 18 c3	35 0538883 E 44 28291 N		Earthquake surface rupture at Akpınar stream locale 4 km north of Ortaoba
YGF-22	H 19 d4	35 0542834 E 44 31164 N		Earthquake surface rupture and sag pond 2 km southwest of Gaybular
YGF-23	H 19 d4	35 0547376 E 44 34888 N	175±15 cm (right lateral)	Offset fence, pressure ridge and linear fault scarp north of Kumköy
YGF-24	H 19 d4	35 0550525 E 44 36293 N	150 cm (right lateral) 10 cm (vertical)	Offset old village road northeast of Muratlar
YGF-25	H 19 d4	35 0550731 E 44 36368 N		Point where surface rupture cuts Muratlar-Gönen road
YGF-26	H 19 d3-d4	35 0553674 E 4437384 N	800±50 m (right lateral)	Total offset of Gönen Stream
YGF-27	H 19 d3	35 0562103 E 44 39833 N		YGF cutting Hallaçlar formation southwest of Kalfaköy
YGF-28	H 19 d3	35 64139 E 44 40556 N	50 cm (vertical)	Surface rupture south of Gökçesu

Figure 6- Linear fault scarp (looking south) (YGF-02) south of Seyvan Village (Photograph taken from Kürçer, 2006).

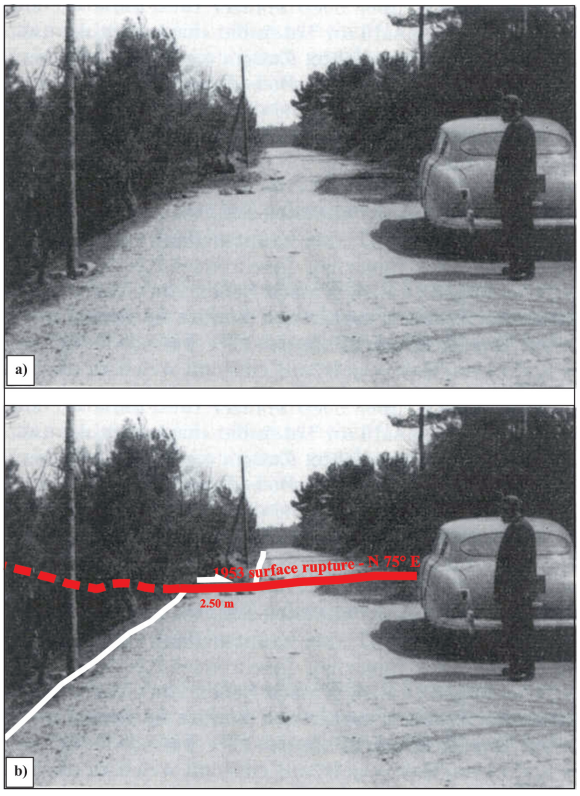

Figure 7- Offset due to the YGE surface rupture on the Yenice – Gönen road (photograph taken from Ketin and Roesly, 1953) (YGF-03) (View to the east).

Village and the north block fell down nearly 50 cm. The strike of the surface rupture between Karasu and Karasukabaklar village was N50°E. Within Karasukabaklar Village, a N70°W surface rupture developed during the 1953 earthquake. This rupture is interpreted as an R fracture developing within a right-lateral strike-slip system.

Northwest of Ortaoba, the Çakır section is separated from the 10 km Gaybular section by a 750 long and 250 m wide step to the left. With N55°E strike, the Gaybular section extends from southwest of Kumköy to Çatalçal Hill and is observed mainly within the Hallaçlar formation in this area, occasionally cutting neritic limestones of the Jurassic-Cretaceous Bilecik formation. The first point in the Gaybular section where the earthquake surface rupture is observed is at Yolçatı locale 2 km north of Karasukabaklar Village (YGF-20 in Table 3). At Yolçatı locale, a surface rupture with N58°E strike developed. The earthquake surface rupture is clearly observed in the northwest slope of Çaltepe 4 km north of Ortaoba. From north of Çaltepe until west of Gaybular, the surface rupture has N60°E strike with a small-scale sag pond occurring in the area northwest of Bozkıraç Hill (YGF-22 in Table 3). The surface rupture forms the contact between the

Jurassic-Cretaceous neritic limestones of the Bilecik formation and the Late Oligocene-Early Miocene Hallaçlar formation in the near southwest of Gaybular Village.

West of Kumköy, the Gaybular section is separated from the Muratlar section with total length of 16 km by a 3 km long and 500 m wide restraining bend. The Muratlar section extends with N65°E strike between Kumköy and Gönen Stream. North of Kumköy in the area of the earthen football pitch (YGF-23 in Table 3), the surface rupture is characterised by offset cultural structures, a small-scale pressure ridge and linear fault scarps.

Between Kumköy and Muratlar, the surface rupture follows the contact between the Hallaçlar formation and Bayramiç formation with N70°E strike and enters ancient alluvial sediments of Gönen River from the north of Muratlar. Ketin and Roesly (1953) reported an old village road east of Muratlar was offset by 1,5 m to the right with the south block falling nearly 10 cm during the YGE (Figure 8) (YGF-24 in Table 3). From here, the surface rupture cuts the Muratlar – Gönen asphalt road with N70°E strike (YGF-25 in Table 3), toward the NE it continues 2 km within alluvial sediments of Gönen River. Just west of Gönen River, Kalaylı Hill rises in the form of a pressure ridge appropriate to the geometry of the fault. The Muratlar section bends 20° to the right from Gönen River to extend toward Çakmak village with E-W strike. In this section, east of Gönen River, the fault cuts the Bayramiç formation and ancient alluvial sediments of the Gönen River in a limited area south of Pilevne and Tirnova neighbourhoods before returning to alluvial sediments until south of Korudeğirmeni. The Muratlar section of the surface rupture enters the Hallaçlar formation south of Korudeğirmeni and continues within this unit west of Çakmak Village where it ends.

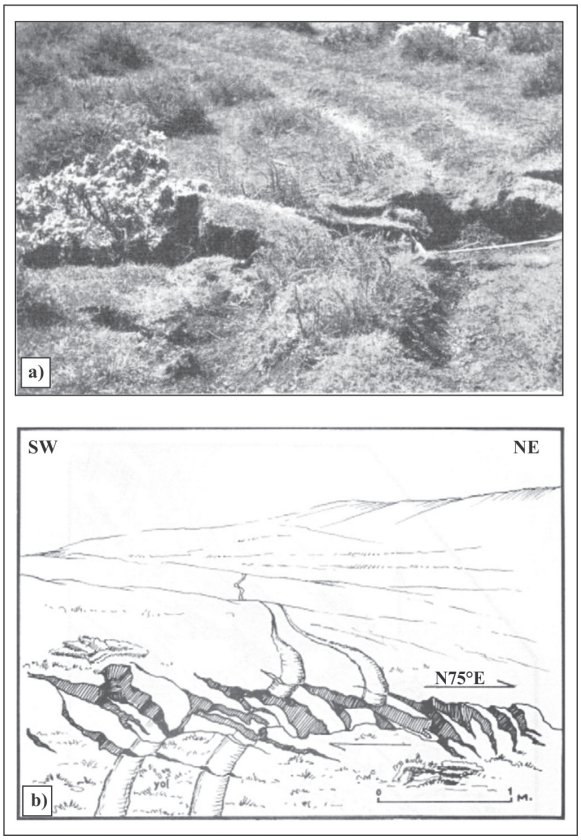

Figure 8- Offset of Muratlar village road during YGE a) Field photograph, b) Sketch (taken from Ketin and Roesly, 1953).

The Kalfaköy section forms the easternmost section of the main body of the YGF. This section extends with strike of N60°E between Korudeğirmeni in the west and Saraçlar in the east. With total length of 6 km, the Kalfaköy section is represented by a deformation zone nearly 300 m wide. The Kalfaköy section ends in a bend toward the SE near Saraçlar village. This section is also equivalent to the region where there is overlap with the surface rupture from the 1964 Manyas earthquake on the YGF (Emre et al., 2012; Kürçer et al., 2017). Most of the Kalfaköy section controls the contact between the Hallaçlar formation and the Bayramiç formation and is occasionally observed within the Bayramiç formation.

The data related to the surface rupture in the Kalfaköy section is limited, but some observations were made that can reveal the structural characteristics of the fault. For example, a nearly 3 m wide crushed and brecciated fault zone was observed southwest of Kalfaköy within the Hallaçlar formation (YGF-27 in Table 3) (Figure 9). From east of Kalfaköy, the fault controls the contact between the Hallaçlar formation and the Bayramiç formation and continues within the Bayramiç formation from south of Gökçesu to reach the Saraçlar bend. South of Gökçesu, the northern block of the earthquake surface rupture fell down nearly 50 cm (YGF-29 in Table 3) and is currently observed as a linear fault scarp (Figure 10). The Saraçlar region represents the easternmost section of the main section of the 1953 YGE surface rupture. In this region, the surface rupture bends toward the SE before continuing 1 km further and ending SE of Saraçlar village. This easternmost 1 km of the surface rupture also ruptured in the 1964 Manyas Earthquake.

Figure 9- YGF cutting Late Oligocene-Early Miocene Hallaçlar formation (Toh) southwest of Kalfaköy (view towards SSW).

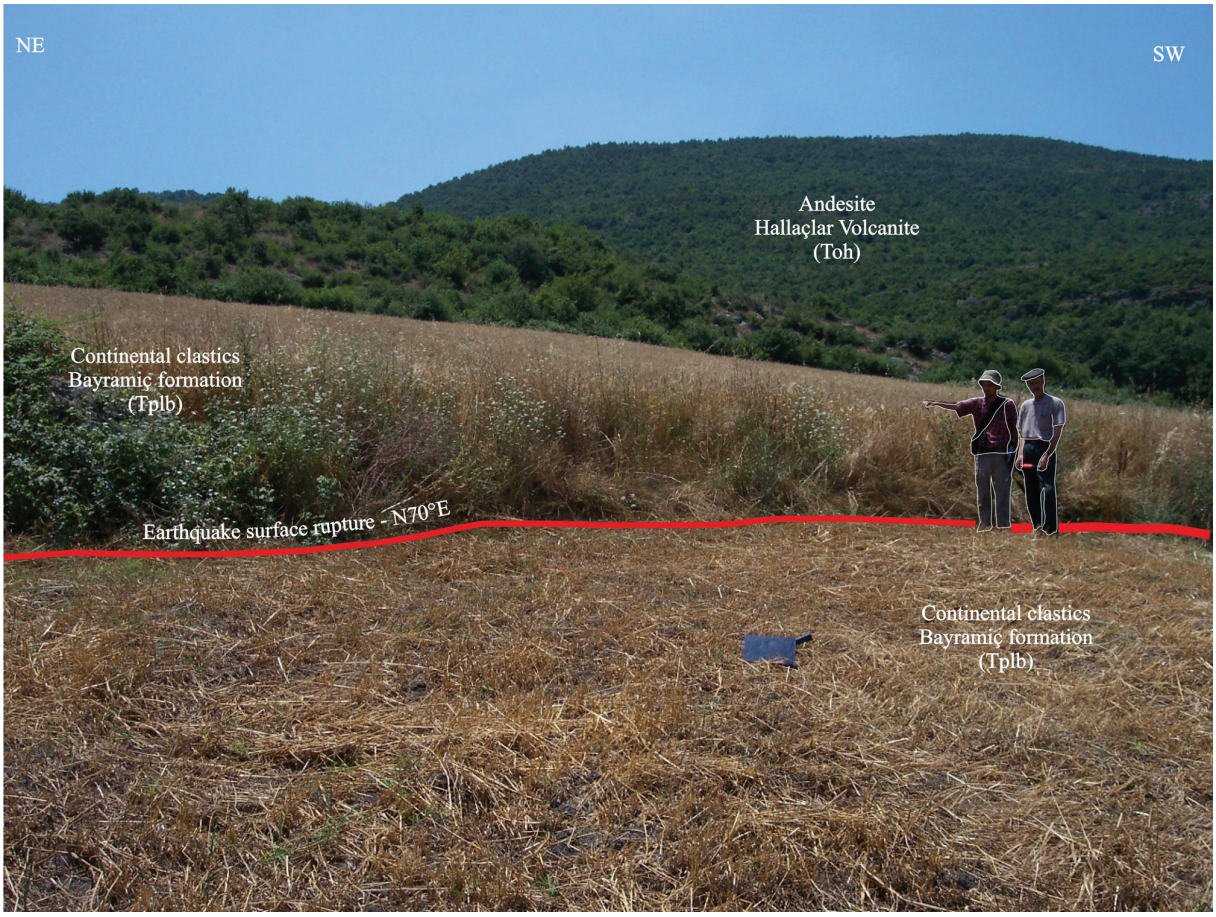

Figure 10- Earthquake surface rupture in the south of Gökçesu village (YGF-24) (Photograph taken from Kürçer, 2006) (view toward SSW).

The 5,5 km section of the YGF extending N70°W between Korudeğirmeni and Koçbayırı villages is named the Tütüncü section. The Tütüncü section is a splay fault separating from the YGF toward the SE (Figure 11). The fault bends toward the left north of Tütüncü and gains a reverse component. Most of the Tütüncü segment controls the contact between the Soma formation and the Bayramiç formation, occasionally cutting the Bayramiç formation and alluvial fan sediments.

5. Offset Measurements the Yenice-Gönen Fault

On the YGE surface rupture, right-lateral displacements varying from 1,70±0,1 m to 3,2±0,2 m were measured (Figure 12, 13 and table 4). Additionally, total displacements varying from 18±2 m and 24±2 m were measured in the Holocene drainage systems in the Çakır section (Figure 13 and 14). The Total station and tape meter were used for these measurement of displacements.

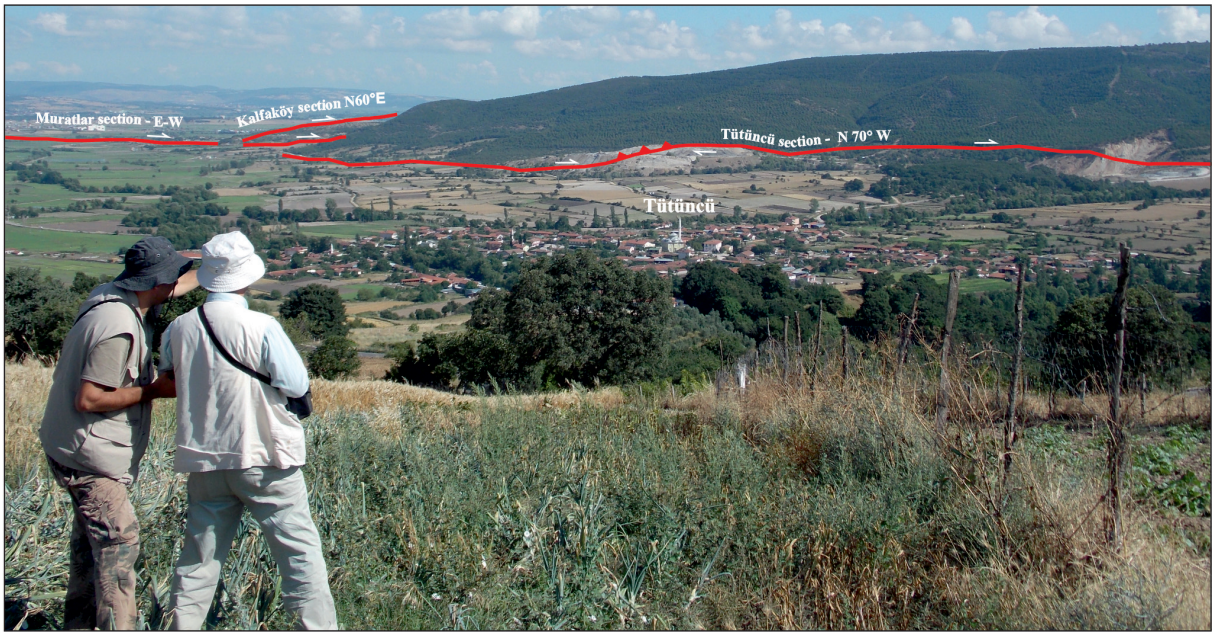

Figure 11- Panoramic view of Tütüncü section of YGF (view north from Tütüncü – Kavakoba road).

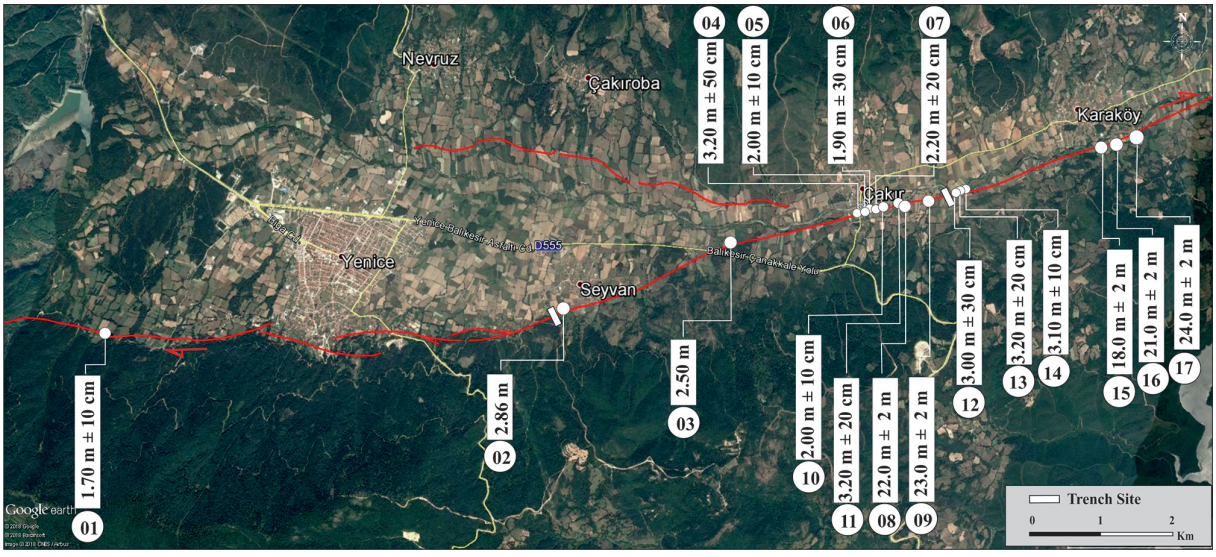

Figure 12- Displacement measurements along the Çakır fault section.

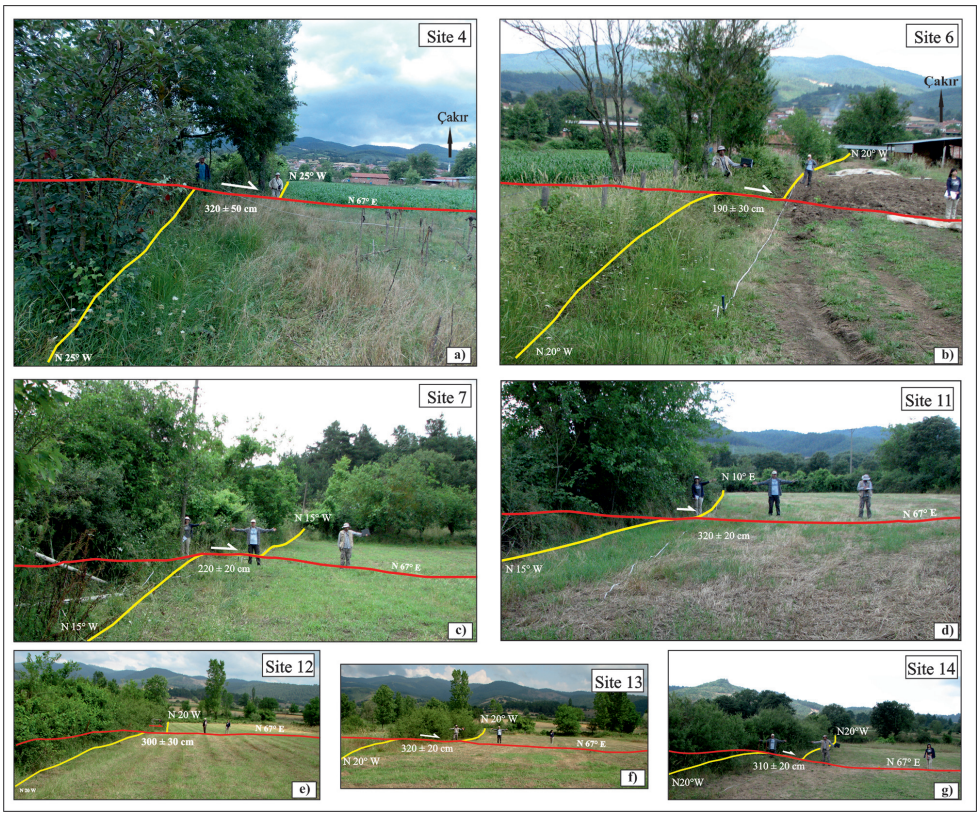

Figure 13- Displacements measured on the YGE surface rupture at some points described in figure 12 and table 4.

Table 4- Displacement measurements along the surface rupture of the YGE.

Station number	Location	Latitude (N)	Longitude (E)	Displacement (m)	Measurement quality	Offset properties and thoughts
01	SW of Yenice	4418504	35 0519481	1,70±10 cm 0,50±5 cm	B	Offset dry stream
02	SW of Seyvan	4419869	35 0525124	2,86	A	Offset dry stream
03	NE of Seyvan	4421120	35 0527125	2,50	A	Yenice – Pazarköy road
04	SSW of Çakır	4421870	35 0528759	3,20±50 cm	C	Field boundary
05	SSW of Çakır	4421884	35 0528786	200±10 cm	A	Field boundary
06	SSW of Çakır	4421884	35 0528801	1,90±30 cm	B	Field boundary
07	SSW of Çakır	4421917	35 0528808	2,20±20 cm	B	Field boundary
08	E of Çakır	4421936	35 0529326	22,00±2 m	B	Offset stream bed (total displacement)
09	E of Çakır	4422075	35 0529653	23,00±2 m	B	Offset stream bed (total displacement)
10	S of Çakır	4421983	35 0528987	2,00±10 cm	A	Field boundary
11	SSE of Çakır	4422035	35 0529263	3,20±20 cm	B	Field boundary
12	SE of Çakır	4422325	35 0529998	3,00±30 cm	A	Field boundary
13	SE of Çakır	4422328	35 0530015	3,20±20 cm	A	Field boundary
14	SE of Çakır	4422358	35 0530053	3,10±10 cm	A	Field boundary
15	SE of Karaköy	4423201	35 531769	18±2 m	B	Offset stream bed (total displacement)
16	SE of Karaköy	4423251	35 531955	21±2 m	B	Offset stream bed (total displacement)
17	SE of Karaköy	4423394	35 532242	24±2 m	B	Offset stream bed (total displacement)
18	N of Kumköy	4434888	35 0547376	1,75±15 cm	B	Field boundary
19	E of Muratlar	4436118	35 0550464	1,50	A	Village road
20	W of Gönen	4437400	35 553605	800±50 m	B	Gönen Stream

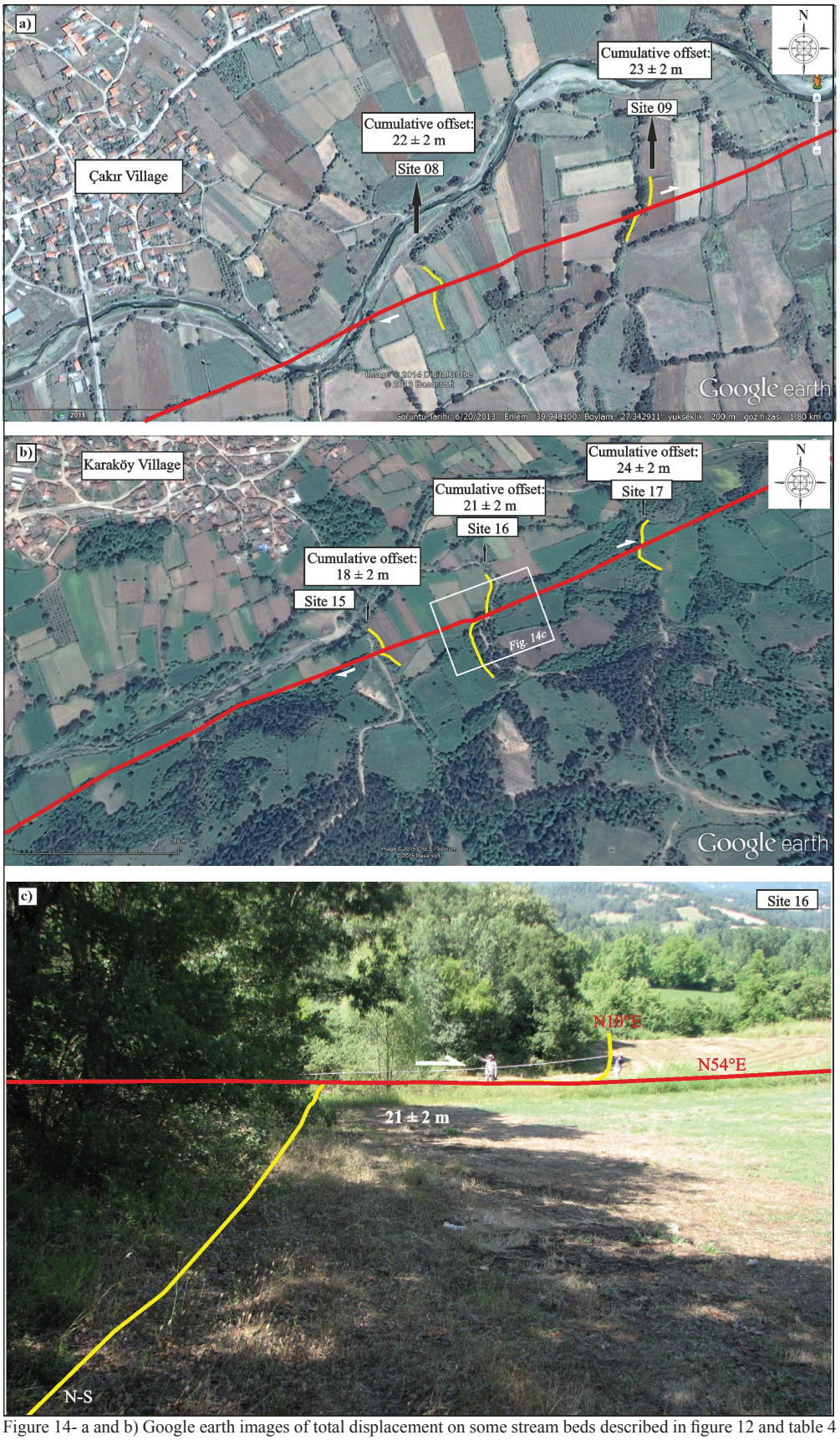

Figure 14- a and b) Google earth images of total displacement on some stream beds described in figure 12 and table 4 along the Çakır fault section, c) Field photograph of station 16.

6. Palaeoseismology Studies

On the Çakır Fault section of the Yenice-Gönen earthquake segment, palaeoseismic trench studies were completed in the Seyvan and Çakır trenches (see figure 12) selected as a result of air photograph analysis and detailed surface rupture mapping. The trench areas firstly had microtopographic maps produced using total station equipment (Figure 16 and 20). All trenches had 1 m^2 gridding applied, and the trench walls were logged with the photomosaic technique. Palaeoseismologic results are presented on sections from the Seyvan 2013-1 trench west wall, Seyvan 2013-2 trench west wall and Çakır 2013 trench west wall.

6.1. Seyvan 2013-1 and Seyvan 2013-2 Trenches

The Seyvan trench area was located 500 m. SW of Seyvan village (UTM coordinates: 35 0525151 E – 4419713 N), SW of Çakır fault section (see figure 12). The Çakır section extending W-E from south of Yenice enters a left restraining bend south of Seyvan and continues to Ortaoba with N67°E strike. In this section the fault gains reverse component due to the effect of the restraining bend (Figure 15).

6.1.1. Site Selection

The clearest data belonging to the surface rupture developing during the 1953 YGE are observed in the Çakır section of the YGF. In this area the 1953 surface rupture is characterised by linear fault scarps. In the Seyvan trench area, a probably Holocene or Late Pleistocene dry stream was cut by the YGF and offset 34±2 m laterally to the right (see figure 13). Ketin and Roesly (1953) measured 4,3 m right lateral displacement on the surface rupture of the 1953 earthquake in Seyvan trench area and surroundings. In this study, right lateral displacements varying from 2,50 m to 3,20 m were measured in Seyvan and close surroundings (see figure 12). From this viewpoint, the total displacement of 34±2 m observed on microtopographic maps is predicted to belong to at least 8 earthquakes. The trench site was chosen with this point of view.

In the Seyvan Trench site, two parallel trenches were excavated perpendicular to the fault and these trenches were named Seyvan 2013-1 trench and Seyvan 2013-2 Trench (Figure 16). Seyvan 2013-1 Trench was 10 m long, mean 3 m deep and 5 metres wide, while Seyvan 2013-2 Trench was 8 m long, 3 m deep and 2 m wide.

6.1.2. Stratigraphy and Structural Patterns

Eleven different microstratigraphic levels were defined in the Seyvan trenches. In both trenches the basement was altered volcanics (volcanic and pyroclastic rocks) from the Late Oligocene-Early Miocene Hallaçlar formation. These units were

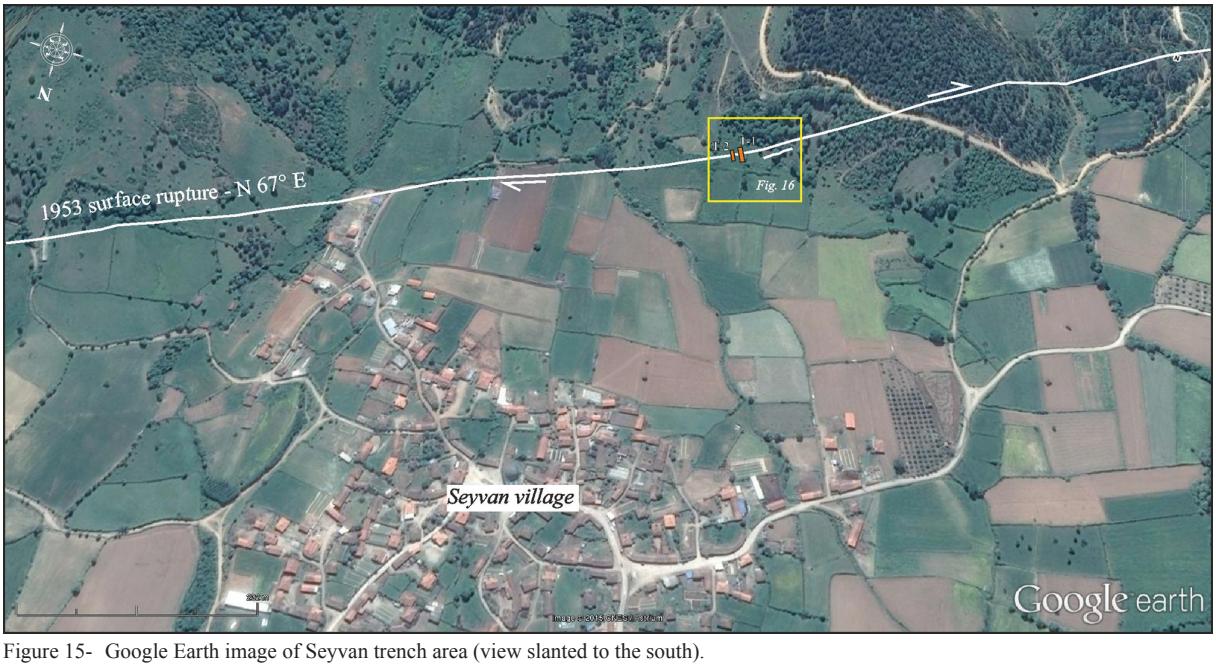

Figure 15- Google Earth image of Seyvan trench area (view slanted to the south).

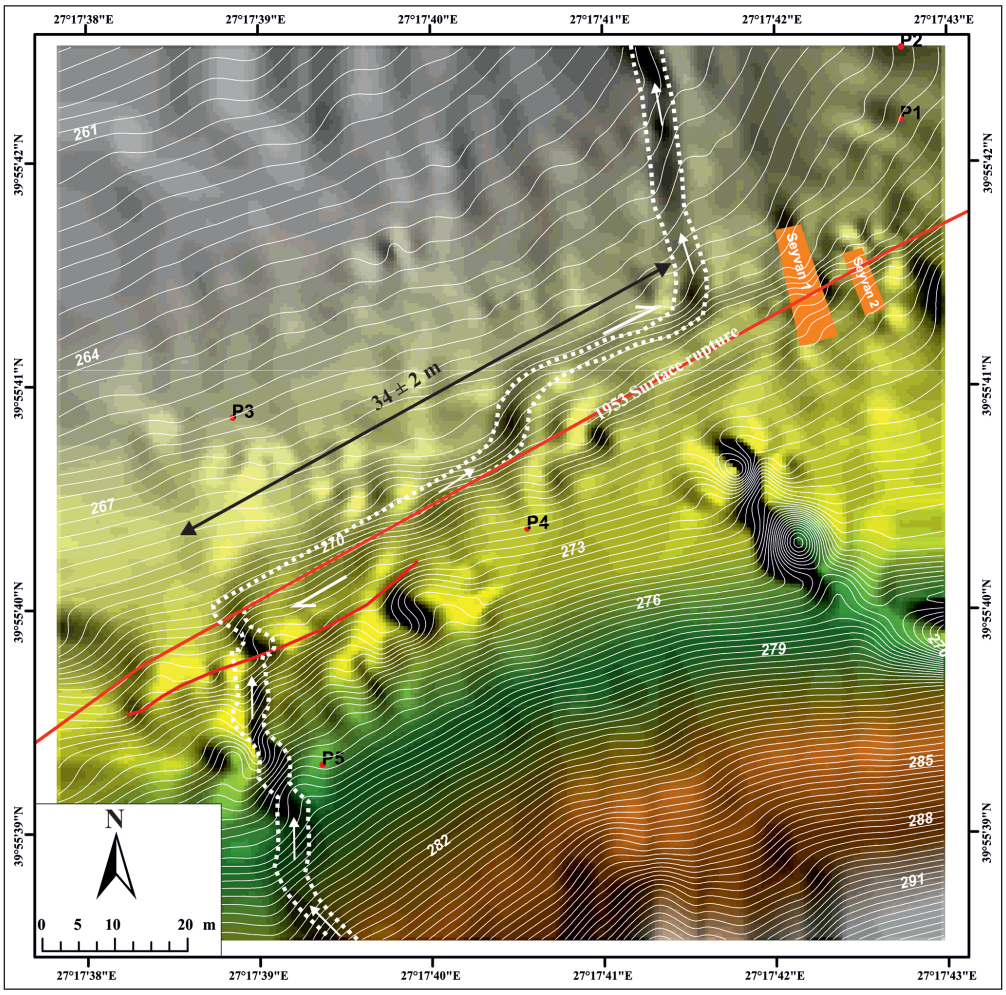

Figure 16- Microtopography map of the Seyvan trench site. Contour interval 20 cm (Kürçer et al., 2016).

unconformably overlain by fan sediments and fault colluvial sediments (Figure 17 and figure 18). In the Seyvan trenches, units numbered 6 and 7 are fault colluvial sediments defining the north of the main fault zone. The structural deformation in the walls of the trenches indicates a transpressive regime. This situation may be explained by the local fault geometry in the trench area.

Considering palaeoseismologic criteria like the tectonostratigraphic relationships between the units, fault colluvial wedge geometry and upward termination of the fault strands, 6 earthquakes resulting in surface ruptures were defined and dated in the Seyvan trenches in the last 6200 years, including the 1953 earthquake. Data belonging to Earthquakes 1, 3, 5 and 6 are present in Seyvan 2013-1 trench, while data for earthquakes 1, 2, 4, 5 and 6 were obtained from Seyvan 2013-2 trench (Figure 17 and Figure 18).

6.1.3. Dating

With the aim of dating the earthquakes identified in the trenches, 20 coal and organic sediment samples were collected and sent to the Beta Analytic Laboratory in the USA for analysis (Table 5). Additionally, 6 sample were collected from levels without carbon-rich material for optically stimulated luminescence dating method (OSL) and these samples were analysed at Ankara University Department of Physical Engineering (Table 6).

6.1.4. Paleoseismologic Interpretation

Earthquake 6: Earthquake 6, which could be determined in both trenches, had an event horizon determined at the base of unit number 5. In Seyvan 2013-1 and 2 trenches, faults north of the main fault zone (between 4th and 5th metres) cut units 1, 2, 3 and 4 and are covered by the gravel in unit number 5.

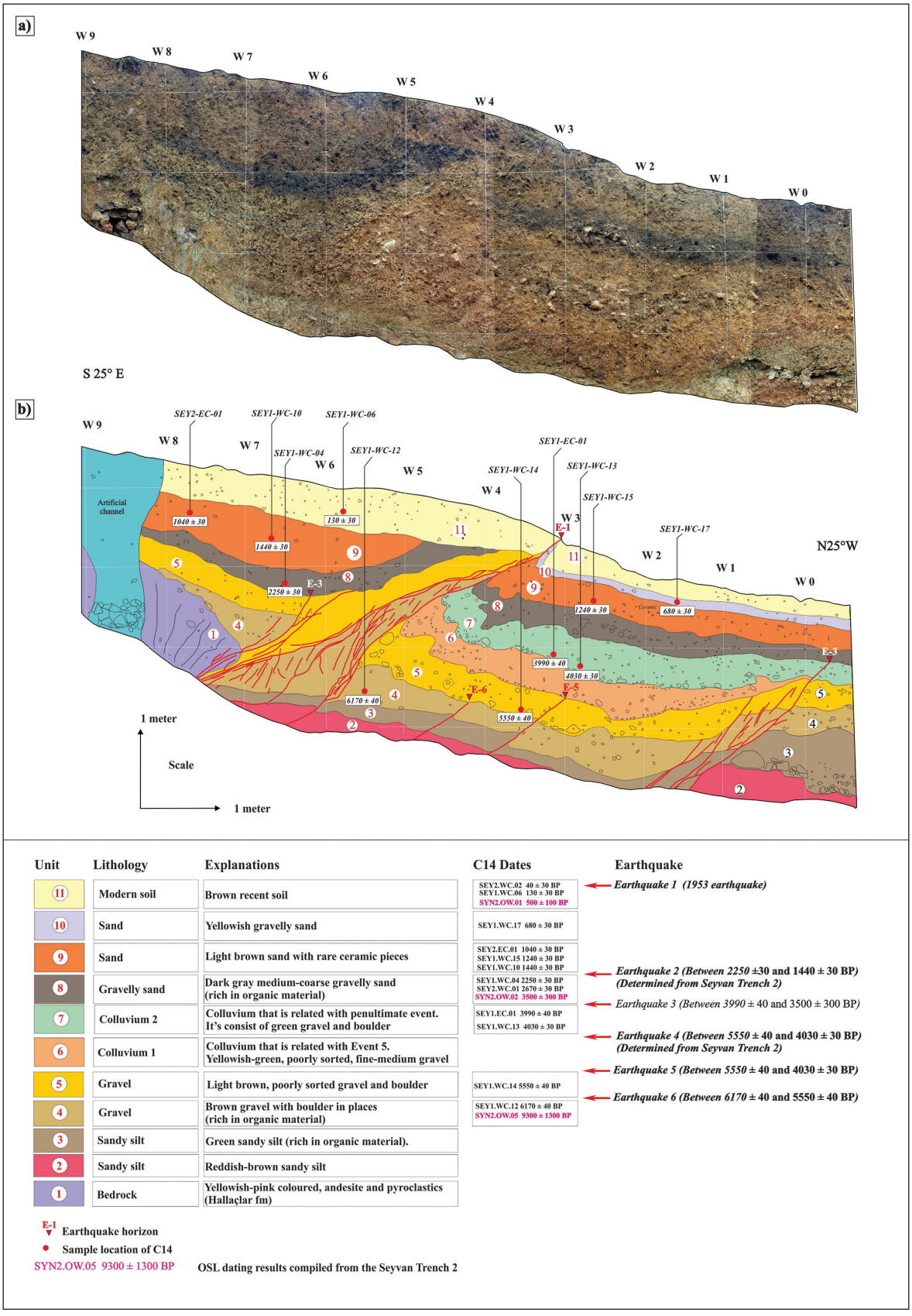

Unit	Lithology	Explanations	C14 Dates	Earthquake
11	Modern soil	Brown recent soil	SEY2.WC.02 40 ± 30 BP SEY1.WC.06 130 ± 30 BP SYN2.OW.01 500 ± 100 BP	← *Earthquake 1 (1953 earthquake)*
10	Sand	Yellowish gravelly sand	SEY1.WC.17 680 ± 30 BP	
9	Sand	Light brown sand with rare ceramic pieces	SEY2.EC.01 1040 ± 30 BP SEY1.WC.15 1240 ± 30 BP SEY1.WC.10 1440 ± 30 BP	← *Earthquake 2 (Between 2250* ±30 and 1440 ± 30 BP*) (Determined from Seyvan Trench 2)*
8	Gravelly sand	Dark gray medium-coarse gravelly sand (rich in organic material)	SEY1.WC.04 2250 ± 30 BP SEY2.WC.01 2670 ± 30 BP SYN2.OW.02 3500 ± 300 BP	← *Earthquake 3 (Between 3990* ± 40 and 3500 ± 300 BP*)*
7	Colluvium 2	Colluvium that is related with penultimate event. It's consist of green gravel and boulder	SEY1.EC.01 3990 ± 40 BP SEY1.WC.13 4030 ± 30 BP	← *Earthquake 4 (Between 5550* ± 40 and 4030 ± 30 BP*) (Determined from Seyvan Trench 2)*
6	Colluvium 1	Colluvium that is related with Event 5. Yellowish-green, poorly sorted, fine-medium gravel		← *Earthquake 5 (Between 5550* ± 40 and 4030 ± 30 BP*)*
5	Gravel	Light brown, poorly sorted gravel and boulder	SEY1.WC.14 5550 ± 40 BP	← *Earthquake 6 (Between 6170* ± 40 and 5550 ± 40 BP*)*
4	Gravel	Brown gravel with boulder in places (rich in organic material)	SEY1.WC.12 6170 ± 40 BP SYN2.OW.05 9300 ± 1300 BP	
3	Sandy silt	Green sandy silt (rich in organic material).		
2	Sandy silt	Reddish-brown sandy silt		
1	Bedrock	Yellowish-pink coloured, andesite and pyroclastics (Hallaçlar fm)		

E-1 Earthquake horizon

Sample location of C14

SYN2.OW.05 9300 ± 1300 BP OSL dating results compiled from the Seyvan Trench 2

Figure 17- a) Uninterpreted photomosaic of the west wall of Seyvan 2013-1 trench b) Trench log of the west wall of Seyvan 2013-1 trench (adapted from Kürçer et al., 2016).

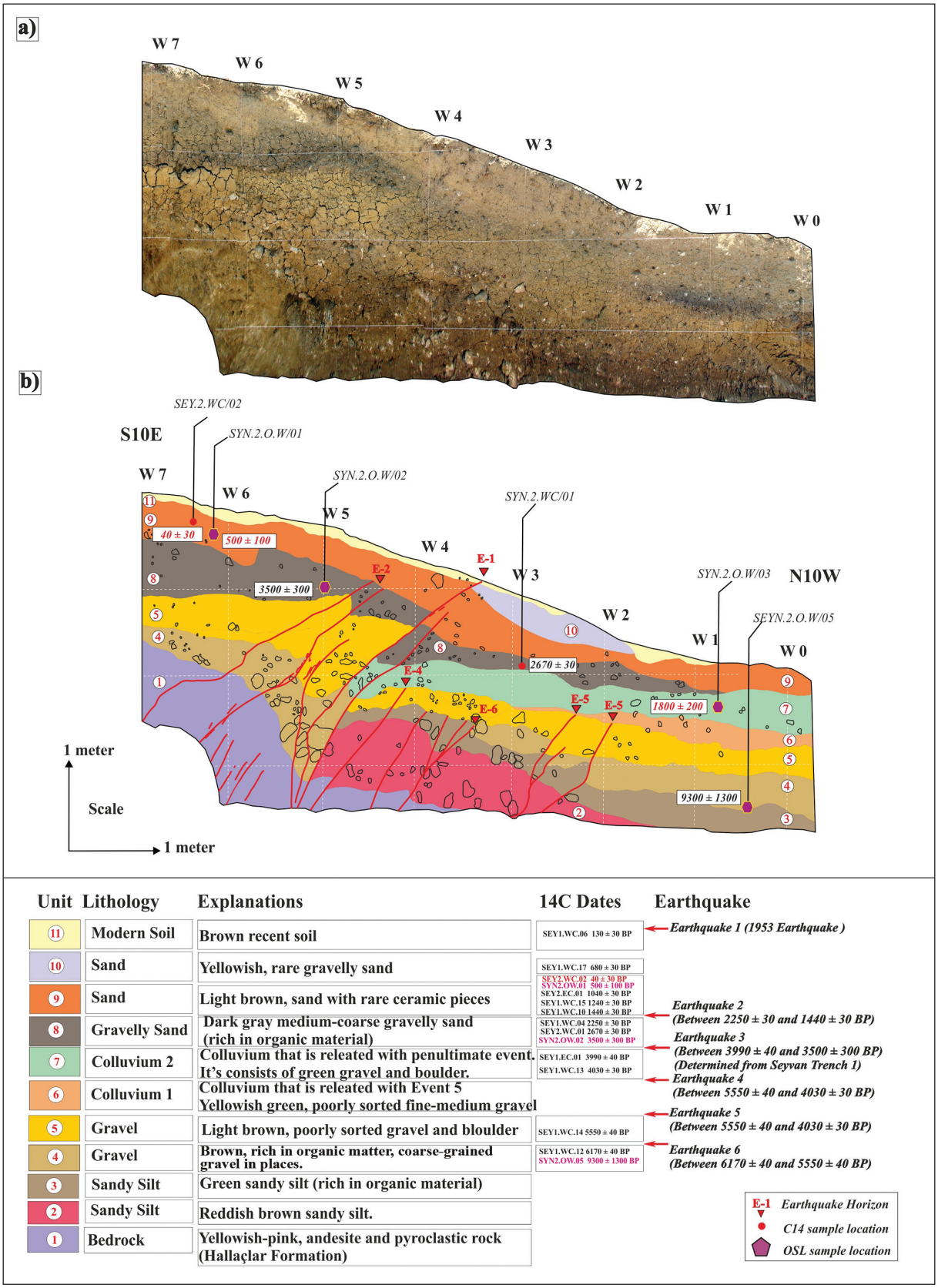

Figure 18- a) Uninterpreted photomosaic of the west wall of Seyvan 2013-2 trench b) Trench log of the west wall of Seyvan 2013-2 trench.

Table 5- Radiocarbon dating results of samples from Seyvan 2013-1, Seyvan 2013-2 and Çakır 2013 trenches.

Trench Wall	Sample No	Laboratory No (BETA)	Stratigraphic unit	Material	Measured radiocarbon age (BP)	^{13}C / ^{12}C (‰)	Traditional radiocarbon age (BP)	Calibrated age interval (2σ)
Çakır 2013- West	CKR-A.W-01	366225	3	Organic sediment	5140±40	-24,0	5160±40	BC 4040 - 4010 BC 4000 - 3940 BC 3860 - 3840 BC 3840 - 3820
Çakır 2013- West	CKR-A.W-02	366226	1	Organic sediment	7050±40	-25,0	7050±40	BC 5980 BC 5940 BC 5920
Çakır 2013- West	CKR-A.W-03	366227	8	Organic sediment	1770±30	-23,9	1790±30	AD 130 - 260 AD 280 - 330
Çakır 2013- West	CKR-A.W-04	366228	4	Organic sediment	3980±30	-24,2	3990±30	BC 2570 - 2460
Çakır 2013- West	CKR-A.W-05	366229	9	Organic sediment	60±30	-25,0	60±30	AD 1690 - 1730 AD 1810 - 1840 AD 1840 - 1850 AD 1860 - 1860 AD 1870 - 1920 AD Post 1950
Çakır 2013- West	CKR-C.W-01	366230	5	Organic sediment	3150±30	-25,0	3150±30	BC 1490 - 1470 BC 1460 - 1390
Çakır 2013-West	CKR-C.W-02	366231	5	Organic sediment	2960±30	-25,0	2970±30	BC 1300 - 1120
Çakır 2013- West	CKR-C.W-04	366232	5	Organic sediment	3260±30	-25,5	3250±30	BC 1610 - 1450
Seyvan 2013-1 - East	SEY.1-EC-01	366233	7	Coalified material	3970±40	-24,0	3990±40	BC 2580 - 2460
Seyvan 2013-1 - West	SEY.1-WC-04	366238	8	Coalified material	2290±30	-27,2	2250±30	BC 390 to 350 BC 320 to 210
Seyvan 2013-1 - West	SEY.1-WC-06	366239	11	Coalified material	160±30	-26,6	130±30	AD 1670 to 1780 AD 1800 to 1900 AD 1900 to 1940 AD 1950 to post 1950
Seyvan 2013-1 - West	SEY.1-WC-10	366241	9	Organic sediment	1420±30	-23,7	1440±30	AD 570 to 650
Seyvan 2013-1 - West	SEY.1-WC-12	366242	4	Organic sediment	6160±40	-24,1	6170±40	BC 5220 to 5000
Seyvan 2013-1 - West	SEY.1-WC-13	366243	7	Organic sediment	4000±30	-23,0	4030±30	BC 2620 to 2470
Seyvan 2013-1 - West	SEY.1-WC-14	366244	5	Organic sediment	5520±40	-23,1	5550±40	BC 4460 to 4340
Seyvan 2013-1 - West	SEY.1-WC-15	366245	9	Organic sediment	1220±30	-23,6	1240±30	AD 680 to 880
Seyvan 2013-1 - West	SEY.1-WC-17	366246	10	Organic sediment	660±30	-23,9	680±30	AD 1270 to 1310 AD 1360 to 1390
Seyvan 2013-2-Doğu	SEY.2-EC-01	366248	9	Organic sediment	1010±30	-23,1	1040±30	AD 900 to 910 AD 970 to 1030
Seyvan 2013-2-West	SEY.2-WC-01	366249	8	Coalified material	2700±30	-26,8	2670±30	BC 890 to 880 BC 850 to 800
Sey Seyvan 2013-2- West	SEY.2-WC-02	366250	11	Coalified material	70±30	-26,8	40±30	AD 1710 to 1720 AD 1830 to 1830 AD 1890 to 1910 AD Post 1950

Table 6- Optically stimulated luminescence (OSL) dating results for samples from Seyvan 2013-1, Seyvan 2013-2 and Çakır 2013 trenches.

Trench Wall	Sample No	Stratigraphic unit	Material	Equal dose (Gy)	Measured OSL age (BP)
Seyvan 2013-2- West	SYN2-OW-01	9	Rough sand	2,1±0,2	500±100
Seyvan 2013-2- West	SYN2-OW-02	8	Pebbly sand	15,5±1,1	3500±300
Seyvan 2013-2- West	SYN2-OW-05	4	Sand	42,7±5,5	9300±1300
Çakır 2013 - West	CKR-OW-03	1	Silty clay	45,4±3,9	7700±800
Çakır 2013 - West	CKR-OW-04	6	Mud	22,5±1,6	3700±300
Çakır 2013 - West	CKR-OW-05	3	Sandy gravel	34,6±4,9	6100±900

The youngest unit cut by faults related to Earthquake 6 is unit number 4 with age dates obtained as 6170±40 years BP. The youngest age obtained above the event horizon (between unit number 4 and 5) is 5550±40 years BP. According to this stratigraphy and age data, the predicted earthquake date for Earthquake 6 is determined to be between 6170±60 BP and 5550±40 BP.

Earthquake 5: Data belonging to Earthquake 5 were found in both trenches. The event horizon for this earthquake was determined to be based in unit number 6. Faults north of the main fault zone between the 2nd and 4th metres in Seyvan 2013-1 and 2 trenches cut all units up to unit number 5 and are covered by colluvial sediments of unit number 6. The youngest age obtained from unit number 5 is 5550±40 years BP. Though age dates could not be obtained from colluvial sediments in unit number 6 covering Earthquake 5, an age of 4030±30 years BP was obtained from the base level of unit number 7 above this. In this situation, the estimated earthquake date for Earthquake 5 is between 5550±40 years and 4030±30 years BP.

Earthquake 4: Evidence of this event was present between the 4th and 5th meters of Seyvan 2013-2 Trench. The event horizon for Earthquake 4 was determined at the base of unit number 7. The youngest unit cut by a fault belonging to this earthquake was unit number 6 and no age dates could be obtained. As a result, the lower age for the earthquake can be given as 5550±40 BP obtained from unit number 5. The youngest age obtained from unit 7 covering unit 6 is 4030±30 years BP. According to this age data, the estimated earthquake date for Earthquake 4 can be given as between 5550±40 years and 4030±30 years BP, similar to Earthquake 5.

Earthquake 3: Earthquake 3 can be clearly distinguished in Seyvan 2013-1 trench. The dark grey coloured pebbly-sand (unit number 8) observed as a marker level in the trench walls forms the event horizon for this earthquake. Two fault branches north and south of the main fault zone end at the base of unit number 8. With the aim of dating the earthquake, the date of 3990±40 years BP was obtained from unit number 7, the youngest unit cut by the fault. Both OSL and C-14 dates were obtained from unit number 8 covering the event horizon. The OSL age obtained from a level close to the base of this unit was 3500±300 years. According to this stratigraphy and age data, Earthquake 3 must have occurred between 3990±40 and 3500±300 years BP.

Earthquake 2: According to Seyvan 2013-2 trench, the event horizon for Earthquake 2 was determined as the base of unit number 9. In Seyvan 2013-2 trench, two faults south of the main fault zone (between 4th and 5th metres) cut unit number 8 and are covered by unit number 9. The youngest age obtained from unit number 8 is 2250±30 years BP. The base of unit 9 covering the event horizon is 1440±30 years BP. According to this data, Earthquake 2 must have occurred between 2250±30 and 1440±30 years BP.

Earthquake 1 (1953 Earthquake): The surface rupture of the 1953 earthquake is clearly observed in both trenches. In the first trench the 1953 earthquake is represented by a narrow deformation zone, while in the second trench there are two fault branches visible. The age obtained from the youngest unit cut by the 1953 earthquake surface rupture is 130±30 years BP.

6.2. Çakır 2013 Trench

The Çakır trench site is located in the central part of the Çakır fault section (see figure 12). The Çakır fault section extends trending N67°E after a restraining bend to the left south of Seyvan and continues within flood plain sediments of the Yenice Stream from south of Çakır to Güzeloba village (see figure 3). In this section the fault is characterised by unique topography of right-lateral strike-slip faulting. Displacements in this section related to the 1953

Figure 19- Google Earth image of Çakır trench site (Oblique view toward the south).

earthquake and total displacements of the Holocene drainage system were measured (see figure 14). The Çakır trench site is located 1250 m ESE of Çakır village (UTM coordinates: 35 05299973 E – 4422153 N; figure 19).

6.2.1. Site Selection

In this area, field boundaries are systematically displaced by the 1953 earthquake surface rupture. The Çakır trench site and surroundings had 300±30 cm to 320±30 cm right lateral displacements measured during the 1953 YGE (see figure 13). Additionally, east and west of the Çakır trench site, right lateral total displacements of 18±2 m and 24±2 m were measured in the Holocene drainage system (see figure 12). The Çakır trench site, where systematic field boundary offsets are clearly observed, is located on flood plain sediments of Yenice Stream. With the aim of determining microtopographic properties of the Çakır trench area, total station equipment was used to produce microtopographic maps (Figure 20). In the Çakır trench site and surroundings, field boundaries systematically offset during the 1953 earthquake are present. These offsets can be clearly observed on microtopographic maps with 20 cm contour intervals produced using the total station (Figure 20).

In the Çakır trench site, one trench was excavated with 10 m length, mean 2,5 m depth and 5 m width perpendicular to the fault.

6.2.2. Stratigraphy and Structural Patterns

The 9 different microstratigraphic levels, were defined in Çakır 2013 trench. Most of these units consists of flood plain sediments of Yenice Stream and partly fault colluvial sediments (Figure 21). The style of structural deformation in the Çakır Trench indicates strike-slip deformation. The faults have transpressive character linked to the local fault geometry in the trench site (Figure 21).

6.2.3. Dating

With the aim of dating the earthquakes identified in the Çakır trench, 8 radiocarbon and 3 OSL samples were reviewed and analysed. For the analysis results, please see table 5 and table 6.

6.2.4. Paleoseismologic Interpretation

Based on the paleoseismological criteria, 5 paleo earthquakes, resulting in surface rupture, were identified and dated within the last 7000 years in Çakır Trench site (Figure 21).

Earthquake 5: At the 6th metre of the Çakır 2013 trench, the event horizon for Earthquake 5, with typical colluvial wedge geometry, was determined at the base of colluvial unit number 2. A date of 7050±40 years BP was obtained from unit number 1, the youngest unit cut by the fault associated with this

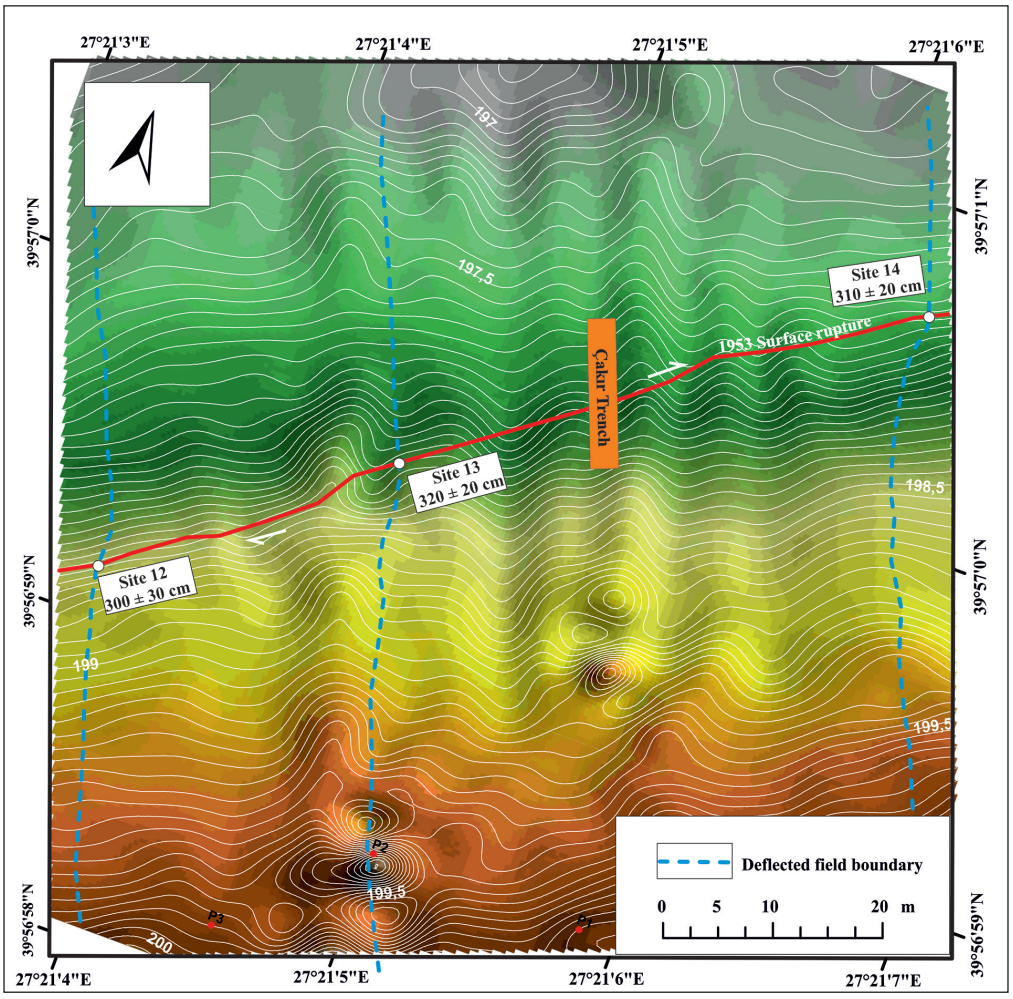

Figure 20- Microtopography map of the Çakır trench site. Contour interval is 20 cm.

event. Though age dates could not be obtained from unit 2 covering this event horizon, an age of 6100±900 years BP was obtained for unit number 3 just above this unit. According to this age data, the recommended age interval for Earthquake 5 is between 7050±40 and 6100±900 years BP.

Earthquake 4: Data belonging to this event are observed between the 7th and 8th metres of this trench. In this section the fault clearly cuts unit number 3 and is covered by unit number 5. As unit number 4 was not observed in the south block of the main fault zone, the event horizon for Earthquake 4 was determined as the base of unit number 5. An age of 3990±30 years BP was obtained from unit number 4. An age of 3250±30 years BP was obtained from the base of unit 5 covering the event horizon. According to this data, the age of Earthquake 4 was determined between 3990±30 and 3250±30 years BP.

Earthquake 3: The event horizon for Earthquake 3 identified in Çakır 2013 trench is at the base of unit number 7. Data belonging to this event are clearly observed between the 4th and 5th metres in the trench. An age of 3700±300 years BP was obtained from unit number 6 under the event horizon. There was no dateable material found in unit number 7 above the event horizon. For this reason, the 1790±30 year BP age date obtained from unit number 8 above this unit was used. Accordingly, the date for Earthquake 3 is proposed to be between 3700±300 and 1790±30 years BP.

Earthquake 2: Clearly observed between the 4th and 5th metres in the trench, the event horizon for Earthquake 2 was determined as the base of unit number 8. As no age data could be obtained for unit number 7, the recommended dates for Earthquake 3 of 3700±300 to 1790±30 years BP were adopted for Earthquake 2.

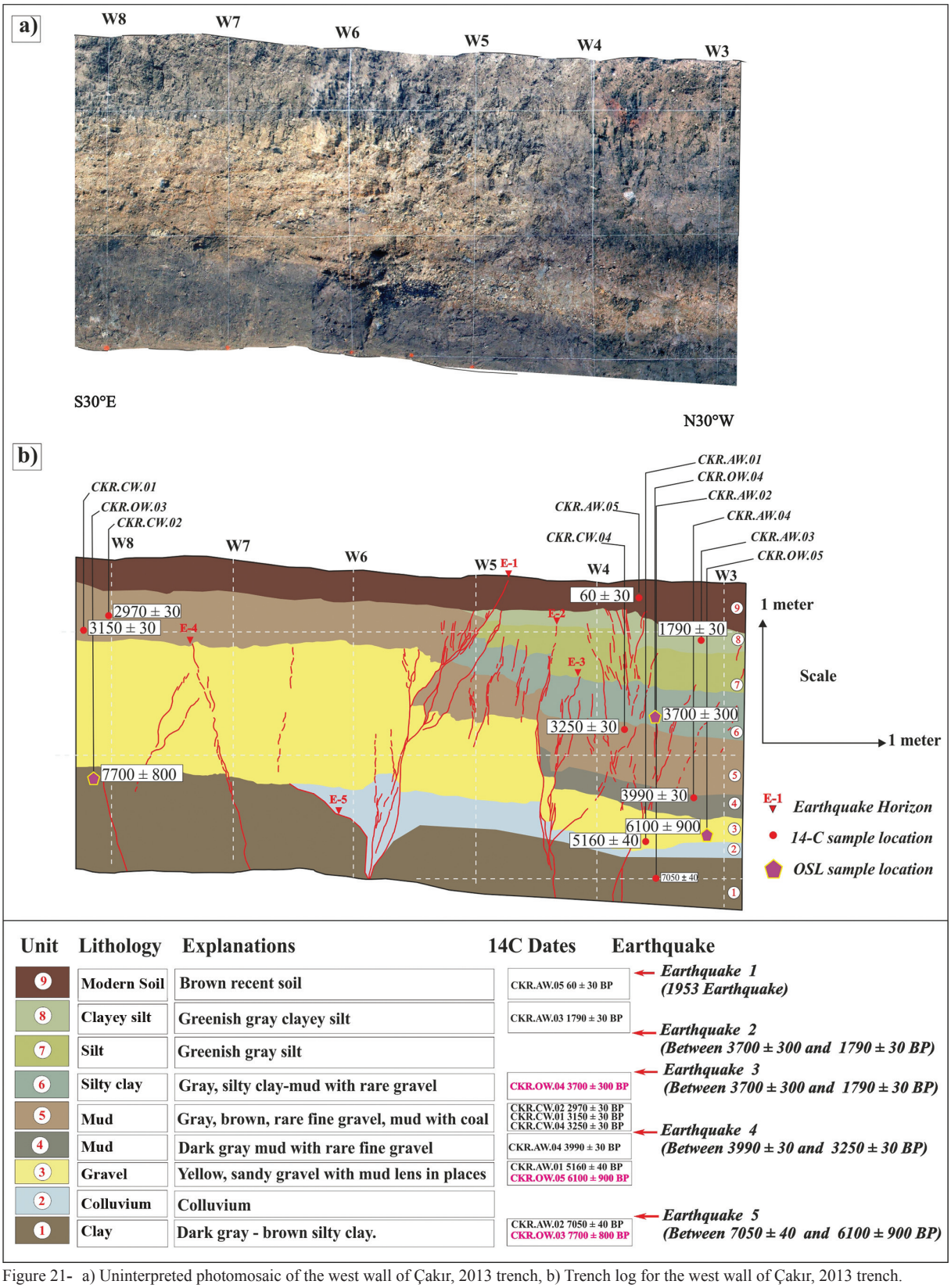

Figure 21- a) Uninterpreted photomosaic of the west wall of Çakır, 2013 trench, b) Trench log for the west wall of Çakır, 2013 trench.

Earthquake 1 (1953 Earthquake): The surface rupture of the 1953 YGE can be clearly observed in Çakır 2013 trench. The main fault branch extends upwards and cuts very young current soil levels dated to 60±30 years BP.

6.3. Comparison of Seyvan and Çakır Trenches

As a result of evaluating the identified and dated earthquakes from the Seyvan (2013-1 and 2013-2) and Çakır 2013 trenches together, a total of 6 earthquakes that resulted in surface rupture were identified and dated on the YGF in the last 6200 years, including the 1953 earthquake (Figure 22). The evaluation of these earthquakes is presented in the Discussion and Conclusion section.

7. Evaluation of Total Offset, Annual Slip Rate (Late Quaternary-Present) and Age of the Yenice-Gönen Fault

For the first time in this study, the total offset and annual slip rate of the YGF was calculated for the last 300.000 years (Late Quaternary) to the present day. The data indicating the total offset of the YGF in the Late Quaternary comes from Gönen River. West of Gönen, Gönen River is cut by the YGF and offset 800±50 m right-laterally (Figure 23). Kazancı et al. (2014) stated the excavation times for large valleys in the South Marmara Region could not go back further than 300,000 years to erosion and deposition rates. This study accepted the incision time for Gönen River

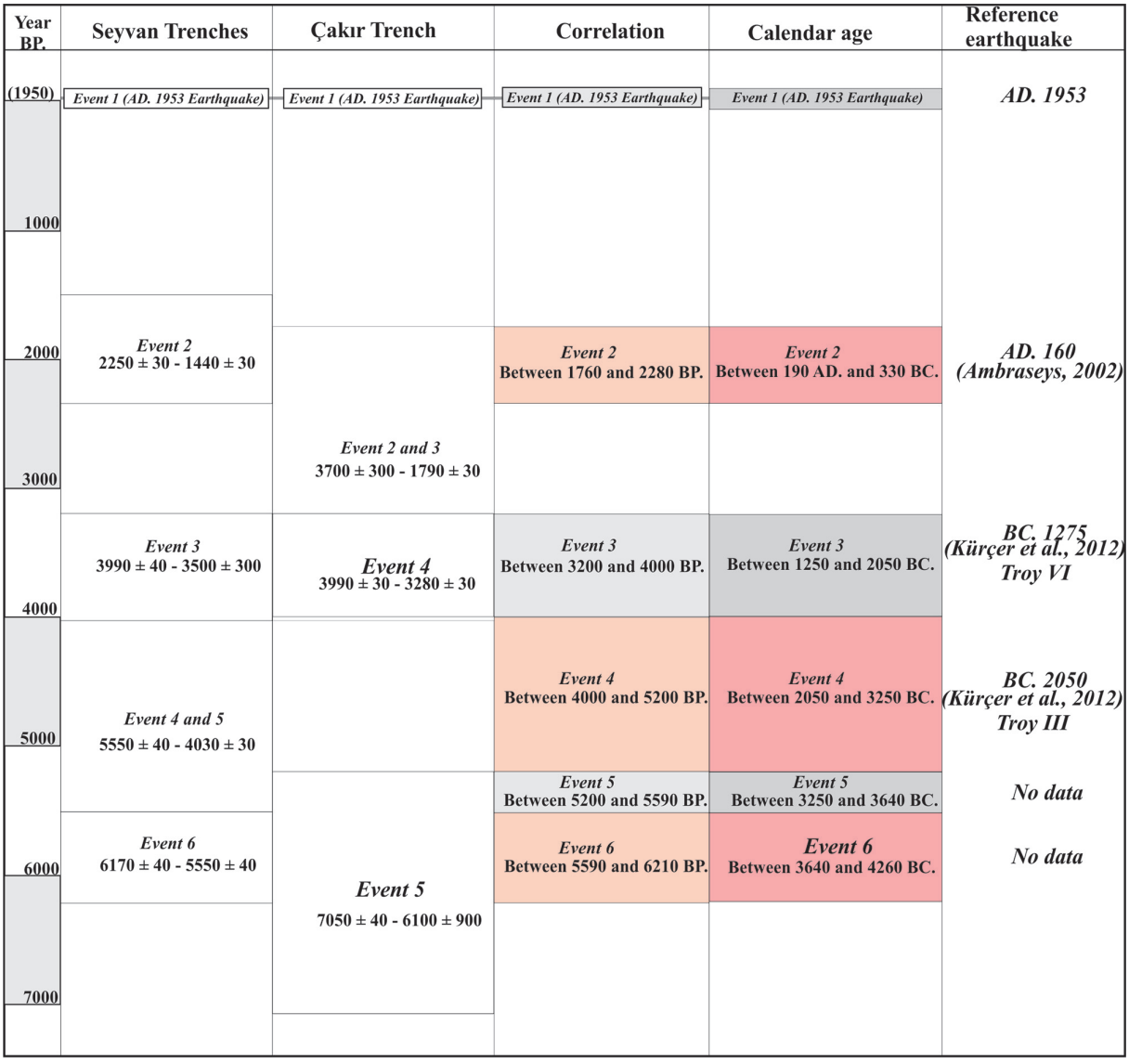

Figure 22- Comparison of earthquakes identified and dated in the Seyvan and Çakır trenches.

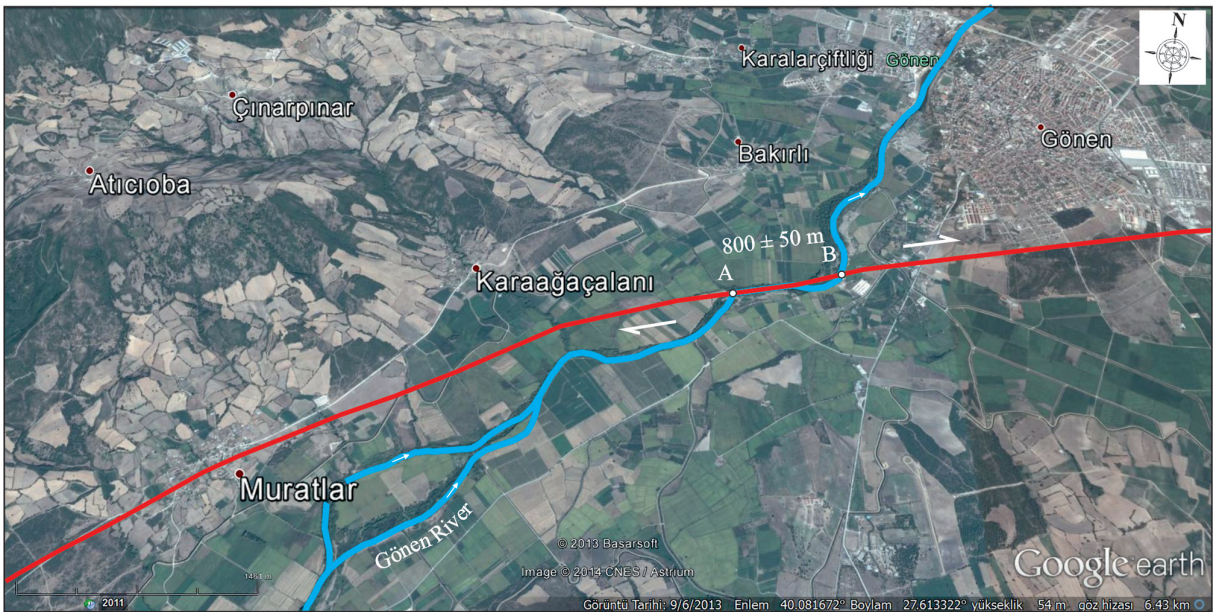

Figure 23- Google Earth image of total displacement on the Gönen River.

as 300,000 years. Calculations using the incision time for Gönen River (300.000 years) and total displacement amount (800±50) found the annual slip rate on the YGF as 2,65±0,15 mm/year. This value complies with previous studies and regional GPS studies. Current GPS studies show the total annual right-lateral slip rate on active faults with NE-SW trending in the Southern Marmara Region is 6-8 mm (Meade et al., 2002; Kreemer et al., 2004). Emre et al. (2012) proposed the annual slip rate on the YGF was 2-3 mm based on the fact that this value has to be shared between the Yenice-Gönen, Sarıköy and Çan-Biga fault zones.

Gürer et al. (2003) in a study of the neotectonic development of the southeast Marmara region described the region as a transition zone between the NAF zone and the Western Anatolia Extensional system. Selim et al. (2013) reported the southern branch of the NAF was effective on the morphotectonic development of the South Marmara region. Selim and Tüysüz (2013) assessed the Bursa-Gönen depression as a complex basin and stated the basin began opening as a small pull-apart basin in the Late Pliocene and later evolved into a large basin. The geomorphology of the Biga Peninsula where the study area is located began to be shaped by the effect of the Western Anatolia Extensional System from the beginning of the Miocene. In this period, small lacustrine basins like Bayramiç, Çan, Yenice, Kalkım, and Gönen developed under the control of normal or strike-slip normal faults. In these basins, the Çan and Soma Formations, occasionally containing coal, developed from the lacustrine facies in the Middle Miocene, while the Bayramiç formation developed from terrestrial, occasionally fluvial, facies in the Pliocene. The Yenice Basin is initially assessed as forming a half graben in the Upper Miocene-Pliocene with the effect of the Western Anatolia Extensional System. The structural evidence for this tectonic phase is present south of Yenice. Slip data measured on fault planes in Oligo-Miocene aged granites (Tg) south of Yenice document that the Yenice Basin initially developed under the control of oblique-slip normal faults (Figure 24). Later in the process, the right-lateral strike-slip YGF cut the basin sediments.

Additionally, new data was reached about the geological offset of the YGF. In the Yenice area, the Late Oligocene-Early Miocene Hallaçlar formation is cut by the YGF with 4,7±0,3 km right-lateral offset (Figure 25). However, as this offset amount could only be measured linked to a single contact, it is open to debate.

When the annual slip rate (2,65±0,15 mm) calculated for the YGF in this study and the 4,7±0,3 km geological offset are assessed together, the formation age of the YGF is expected to be nearly 1,9 million years. However, as can be clearly seen on Figure 24, the Yenice Basin had a half graben form shaped by strike-slip normal faults initially.

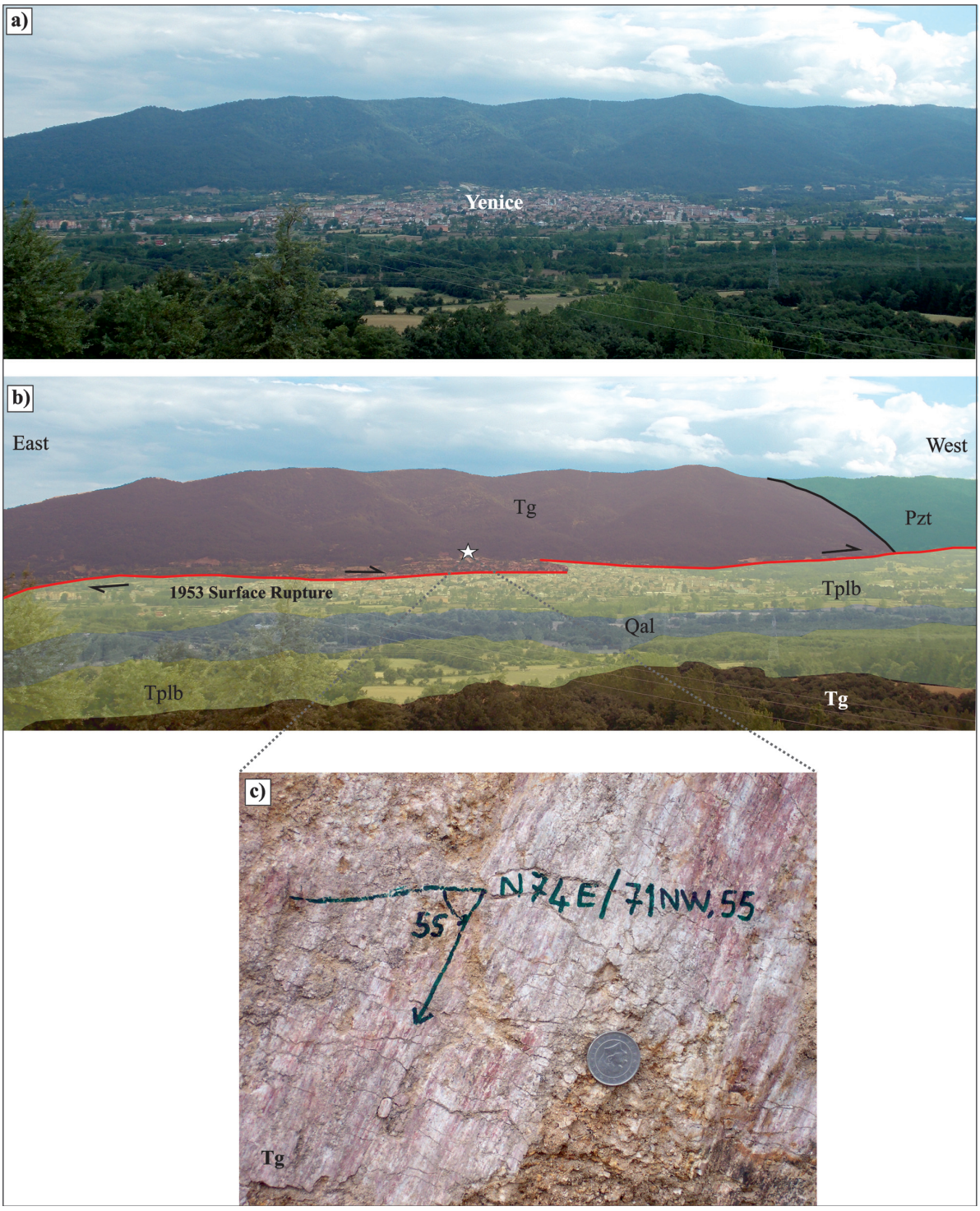

Figure 24- a) Panoramic view of the Yenice Basin, b) Field photograph showing rock units outcropping in the south of the Yenice Basin. For explanations of rock units see figure 3. Star: shows fault plane observation point. c) Oblique slip normal fault plane at the basin edge measured in Tertiary-aged granitoids (Taken from Kürçer, 2006) (view to the south).

As a result, a significant amount of the 4,7±0,3 km geological offset measured in the Late Oligocene-Early Miocene Hallaçlar formation south of Yenice must be associated with the strike-slip normal faulting during basin development. In this situation, the age of the YGF may be assessed as being much younger than 1,9 million years.

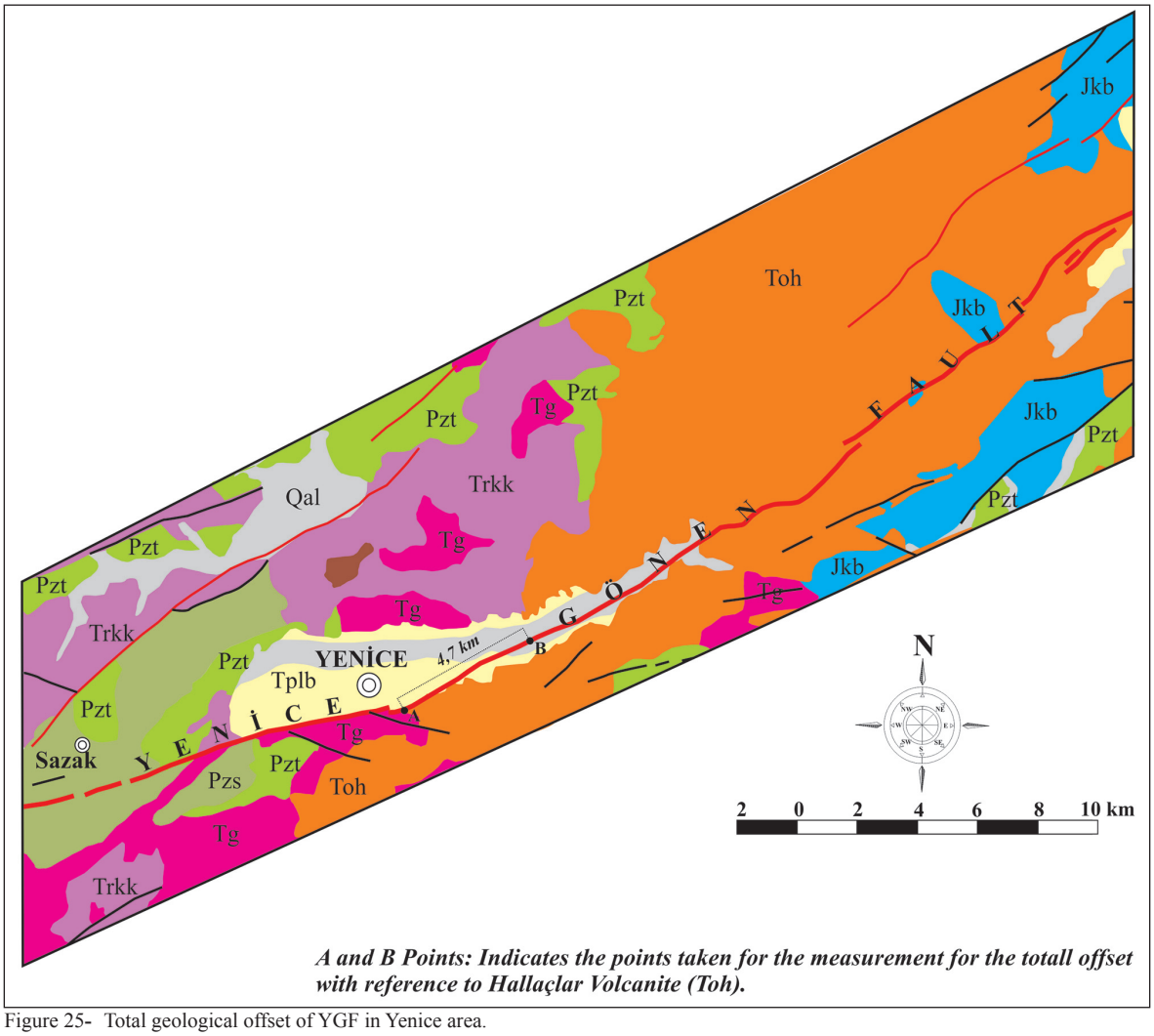

Figure 25- Total geological offset of YGF in Yenice area.

8. Discussion and Conclusions

In this paper, the properties of the 18 March 1953 YGE surface rupture, active tectonics and palaeoseismologic characteristics of the YGF were assessed holistically.

The YGF is an earthquake segment with total length of 70 km comprising 6 fault sections with lengths varying from 5,5 to 19 km separated by releasing or restraining steps or bends (Figure 3 and 4).

Right-lateral displacements varying between 1,70±0,1 m and 3,2±0,2 m were measured on the YGE surface rupture, with the largest displacement of 3,2±0,2 m measured southeast of Çakır village (Figure 12). The displacement amounts show relative reductions in the NE and SW directions, showing the rupture during the 1953 earthquake began NE of Yenice (between Çakır and Karaköy) and generally progressed in both directions toward the NE and partly toward the SW. Total displacement of between 18±2 m and 24±2 m measured in the Holocene drainage system is morphotectonic evidence that the YGF produced earthquakes resulting in surface rupture at least six times during the Holocene.

According to paleoseismology studies on the Çakır fault section of the YGE segment, 6 earthquakes resulting in surface rupture were identified on the YGF in the last 6200 years including the 1953 earthquake. These earthquakes were dated with radiometric methods (^{14}C and OSL) (Figure 22).

As a result of assessing the trenches together, the earthquake (Earthquake 2) before the 1953 earthquake was determined to have occurred between 330 BC and 190 AD and was correlated with the 160 AD

earthquake. In historical earthquake catalogues, there is no historical earthquake data that can be compared with some of the earthquakes (Earthquakes 3, 4, 5 and 6) identified and dated in this study. Additionally, there is archaeological evidence that ancient Troy, located west of the study area and dated to 3000 BC to 400 AD, was destroyed or damaged by ancient earthquakes (Rose, 1994 and 1996). Kürçer et al. (2012) found traces of ancient earthquakes in the remains from layers 3 and 6 in Troy. On an izoseist map for the 1953 YGE (Kalafat et al., 2007), it appears the area around Troy was affected by MSK=VIII (see figure 23 in Kürçer et al., 2012). Earthquakes 3 and 4 identified in this study may be assessed as the earthquakes destroying Troy layers 3 and 6 in Troy. Earthquake 3 is proposed to date to 1275 BC, the final date for Troy layer 6 (1800-1275 BC), and Earthquake 4 is proposed to date to 2050 BC, the final date for Troy layer 3. There is no historical earthquake or archaeological information found for comparison with Earthquakes 5 and 6. The predicted date for Earthquake 5 is between 3250 and 3650 BC. For Earthquake 6, the period from 3640 to 4260 BC is proposed.

According to palaeoseismology studies in Kürçer (2006) and Kürçer et al. (2008) with data obtained from three earthquakes including the 1953 earthquake, the averagely earthquake recurrence interval for the YGF is proposed as 660±160 years. According to the earthquake dates obtained in this study, the YGF has a variable and irregular earthquake recurrence interval from 505 years to 1793 years. Accordingly, the averagely earthquake recurrence interval for the YGF is proposed as 1180 years.

The temporal and spatial proximity of some earthquakes identified in this study (Earthquake 1 and 2) with earthquakes occurring in the instrumental and historical periods in the region is noteworthy (see figure 2). This data point out that historical and instrumental earthquakes occurring on active faults in the region may be caused stress transfer to neighbouring fault segments.

In this paper, the total offset and annual slip rate for the YGF was calculated for the last 300,000 years (Late Quaternary-present). Data illustrating the total offset of the YGF since the Late Quaternary comes from Gönen River. According to erosion and deposition rates, Kazancı et al. (2014) stated the incision times for large valleys in the Southern Marmara region did not extend beyond 300,000 years. Selim et al. (2013) proposed the Gönen River was cut by the YGF and offset by a total of 5,5 km. However, the fault location stated for the YGF in this study (see figure 5 in Selim et al., 2013) is very different to the location known in the literature and adopted in this study. Considering the excavation times for large rivers in the Southern Marmara region do not extend beyond 300.000 years (Kazancı et al., 2014), for the YGF to cause a total of 5,5 km offset on the Gönen River, the annual slip rate on the fault must be 18 mm which does not comply with regional geology, and active fault and geodesy studies. In this study the total displacement amount on Gönen River west of Gönen was measured as 800±50 m (Figure 23). Calculations using the incision time of Gönen River (300.000 years) and total displacement amount (800 ±50 m) found the annual slip rate on the YGF was 2,65±0,15 mm/year. This value complies with previous studies and regional GPS studies. Current GPS studies show the total annual right-lateral slip rate on NE-SW striking active faults located in the Southern Marmara region is 6-8 mm (Meade et al., 2002; Kreemer et al., 2004). Emre et al. (2012) stated that this value must be shared between the Yenice-Gönen, Sarıköy and Çan-Biga fault zones. In this situation, after the YGF, the remaining amount of the 6-8 mm/year slip rate calculated from GPS studies is considered to be shared by other active right-lateral strike-slip faults within the Biga Peninsula led by the Sarıköy and Çan-Biga fault zones.

The geological offset of the YGF was determined as 4,7±0,3 km in the Late Oligocene-Early Miocene Hallaçlar formation near Yenice (Figure 25). When the annual slip rate (2,65±0,15 mm) and 4,7 km geological offset are assessed together, the formation age of the YGF is predicted as 1,9 million years. However, the Yenice Basin began as a half-graben shaped by an oblique-slip normal fault. As a result, a significant portion of the 4,7 km geological offset measured in the Late Oligocene-Early Miocene Hallaçlar formation may be associated with oblique-slip normal faulting during basin development. In this situation, the age of the YGF may be assessed as much younger than 1,9 million years.

Acknowledgements

This study was completed within the scope of the Turkish National Paleoseismology Research Project (TURKPAP). Project no: 2013-30-14-07. We would like to thank sincerely to Prof. Dr. Okan Tüysüz (İstanbul Technical University), Prof. Dr. Hasan Sözbilir (Dokuz Eylül University), Prof. Dr.

Alexandros Chatzipetros (Aristotle University of Thessaloniki) and anonymous referee whose valuable comments and useful criticisms have greatly improved the manuscript.

References

Allmendinger, R. W., Cardozo, N., Fisher, D. 2012. Structural geology algorithms: Vectors and tensors in structural geology. Cambridge University Press, 302 p.

Altunkaynak, Ş., Dilek, Y., Genç, C. Ş., Sunal, G., Gertisser, R., Furnes, H., Yang, J. 2012. Spatial, temporal and geochemical evolution of Oligo–Miocene granitoid magmatism in western Anatolia, Turkey. Gondwana Research, 21 (4), 961-986.

Ambraseys, N.N. 2002. The seismic activity of the Marmara Sea region over the last 2000 years. Bulletin of the Seismological Society of America, 92 (1), 1-18.

Ambraseys, N.N., Finkel, C.F. 1991. Long-term seismicity of İstanbul and of the Marmara Sea region. Terra Nova 3, 527–39

Ambraseys, N., Jackson, J. 2000. Seismicity of the Sea of Marmara (Turkey) since 1500, Geophys. J. Int., 141**,** F1–F6.

Armijo, R., Meyer, B., Hubert-Ferrari, A., Barka, A. 1999. Westward propagation of North Anatolian Fault into the Northern Aegean: timing and kinematics. Geology, 27, 267–70

Ayhan, E. E., Alsan, N., Sancaklı, S.B., Üçer, B. 1981. Türkiye ve Dolayları Deprem Kataloğu (1881-1990). Boğaziçi Üniversitesi Yayınları, 126 s.

Aysal, N. 2015. Mineral chemistry, crystallization conditions and geodynamic implications of the Oligo–Miocene granitoids in the Biga Peninsula, Northwest Turkey. Journal of Asian Earth Sciences, 105, 68-84.

Aysal, N., Ustaömer, T., Öngen, S., Keskin, M., Köksal, S., Peytcheva, I., Fanning, M. 2012*a*. Origin of the Early-Middle Devonian magmatism in the Sakarya Zone, NW Turkey: geochronology, geochemistry and isotope systematics. Journal of Asian Earth Sciences, 45, 201-222.

Aysal, N., Öngen, S., Peytcheva, I., Keskin, M. 2012*b*. Origin and evolution of the Havran Unit, Western Sakarya basement (NW Turkey): new LA-ICP-MS U-Pb dating of the metasedimentary-metagranitic rocks and possible affiliation to Avalonian microcontinent. Geodinamica Acta, 25 (3-4), 226-247.

Barka, A.A., Kadinsky-Cade, K. 1988. Strike-slip fault geometry in Turkey and its influence on earthquake activity. Tectonics, 7 (3), 663–684.

Barka, A., Gülen, L. 1988. New constrains on age and total offset on the North Anatolian Fault Zone: Implications for tectonics of the Estern Mediterranean Region. METU Journal of Pure and Applied Sciences, 21, 39–63.

Barka, A., Akyüz., S., Altunel, E., Sunal., G., Çakır, Z., Dikbaş, A., Yerli, B., Armijo, R., Meyer, B., de Chabalier, J. B., Rockwell, T., Dolan, J.R., Hartleb, R., Dawson, T., Christofferson, S., Tucker, A., Furnal, T., Langridge, R., Stenner, H., Lettis, Bachhuber, J., ve Page, W. 2002. The Surface Rupture and Slip Distribution of the 17 August 1999 İzmit Earthquake (M 7.4), North Anatolian Fault. Bull. Seism. Soc. Amer. 92 (1): 43-60.

Bozkurt, E. 2001. Neotectonics of Turkey – A synthesis. Geodinamica Acta, 14, 3–30.

Canıtez N, Üçer S.B. 1967. A Catalogue of Focal Mechanism Diagrams for Turkey and Adjoining Areas. İTÜ Maden Fak., Arz Fiziği Enst. Yayın No. 25. 111 pp.

Dirik, K., Belindir, F., Özsayın, E., Kutluay, A. 2008. Neotectonic features and paleoseismology of Yenice- Gönen Fault Zone. Final report of TUBİTAK. Report no: TUJJB-UDP04-02, Ankara.

dePolo, C. M., Clark, D. G., Slemmons, D. B., Aymand, W. H. 1989. Historical Basin and Range Province surface faulting and fault segmentation. In Fault Segmentation and Controls of Rupture Initiation and Termination (D. P. Schwartz, and R. H. Sibson, Eds.), U.S. Geol. Surv. Open File Rep. 89–315, pp. 131–162.

dePolo, C. M., Clark, D. G., Slemmons, D. B., Ramelli, A. R. 1991. Historical surface faulting in the Basin and Range Province, western North America—Implications for fault segmentation. J. Struct. Geol. 13, 123–136.

Duru, M., Pehlivan, Ş., Okay, A.İ., Şentürk, Y., Kar, H. 2012. Biga Yarımadası'nın Tersiyer Öncesi Jeolojisi. Yüzer, E. ve Tunay, G. (Ed.), Biga Yarımadası'nın Genel ve Ekonomik Jeolojisi (7-74). Ankara: ISBN: 978-605-5310-18-9. Maden Tetkik ve Arama Genel Müdürlüğü Özel Yayın Serisi 28, 7-74.

Emre, Ö., Doğan, A., Yıldırım, C. 2012. Biga Yarımadasının diri fayları ve deprem potansiyeli. In: Yüzer, E. ve Tünay, G. (Eds.), Biga Yarımadası'nın Genel ve Ekonomik Jeolojisi, Maden Tetkik ve Arama Genel Müdürlüğü Özel Yayın Serisi 28, 163-198, Ankara-Türkiye.

Emre, Ö., Duman, T. Y., Özalp, S., Elmacı, H., Olgun, Ş., Şaroğlu, Ş. 2013. Açıklamalı Türkiye Diri Fay Haritası, Maden Tetkik ve Arama Özel Yayın Serisi 30.

GCMT Catalogue. The Harvard Centroid Moment Tensor Ctaloque. The Global Centroid-Moment Tensor (CMT) Project, 1976-2012, http://globalcmt.org7

Gürer, Ö.F., Kaymakçı, N., Çakır, Ş., Özburan, M. 2003. Neotectonics of the southeast Marmara region, NW Anatolia, Turkey. Journal of Asian Earth Sciences 21, 1041–1051.

Harvard Univ. 1998. Dep. Earth Planet. Sci., Cambridge, MA. http://www.seismology.harvard.edu

Herece, E. 1990. 1953 Yenice–Gönen deprem kırığı ve Kuzey Anadolu fay sisteminin Biga Yarımadası'ndaki uzantıları, Maden Tetkik ve Arama Dergisi, 111, pp. 47–59.

Jackson, J., McKenzie, D.P. 1984. Active tectonics of the Alpine–Himalayan Belt between western Turkey and Pakistan. Geophys. J. R. Astron. Soc., 77, 185–246.

Karacık, Z., Yılmaz, Y., Pearce, J. A., Ece, Ö. I. 2008. Petrochemistry of the south Marmara granitoids, northwest Anatolia, Turkey. International Journal of Earth Sciences, 97 (6), 1181-1200.

Karakaisis, G. F., Papazachos, C. F., Scordilis, E. M. 2010. Seismic sources and main seismic faults in the aegean and surrounding area, Bulletin of the Geological Society of Greece. Proceedings of the 12th International Congress (pp. 2016–2042). Patras.

Kazancı, N., Emre, Ö., Erturaç, K., Leroy, S.A.G., Öncel, S., İleri, Ö., Toprak, Ö. 2014. Possible incision time of the large valleys in southern Marmara region, NW Turkey. Maden Tetkik ve Arama Dergisi 148, pp. 1–17.

Ketin, I., Roesly, F. 1953. Makroseismische Untersuchungen über das nordwestanatolische Beben vom 18. Marz 1953. Eclogae Geol. Helv. 46, 187–208.

Kocaefe, S., Ataman, G. 1976. Anadolu'da sismotektonik olaylar: Antalya-Fethiye-Denizli üçgeni içinde yer alan bölgenin incelenmesi. Hacettepe Univ. Yerbilim. Derg. 2, 55–70

Kreemer, C., Chamot-Roke, N., Le Pichon, X. 2004. Constraints on the evolution and vertical coherency of deformation in the North Aegean from a comparison of geodetic, geologic and seismologic data. Earth Planet. Sci. Lett. 225, 329–346.

Kürçer, A. 2006. Yenice Gönen Civarının Neotektonik Özellikleri ve 18 Mart 1953 Yenice Gönen Deprem (Mw=7.2) Fayı'nın Paleosismolojisi, KB Türkiye. Yüksek Lisans Tezi, Tez No: 185774, Çanakkale Onsekiz Mart Üniversitesi, Fen Bilimleri Enstitüsü, 190 sayfa (unpublished).

Kürçer, A. 2008. Yenice Gönen Fayı ve sismotektonik anlamı, KB Anadolu, Türkiye. Ulusal Jeomorfoloji Sempozyumu, Bildiriler, 213-214. Çanakkale, 2008.

Kürçer, A. 2012. Tuz Gölü Fay Zonu'nun Neotektonik Özellikleri ve Paleosismolojisi, Orta Anadolu, Türkiye, Doktora Tezi, Tez No: 318203, Ankara Üniversitesi, Fen Bilimleri Enstitüsü, 318 sayfa (unpublished).

Kürçer, A., Chatzipetros, A., Tutkun, S. Z., Pavlides, S., Ateş, Ö., Valkaniotis, S. 2008. The Yenice–Gönen active fault (NW Turkey): Active tectonics and palaeoseismology. Tectonophysics, 453, 263–275.

Kürçer, A., Chatzipetros, A., Tutkun, S. Z., Pavlides, S., Özden, S., Syrides, G., Vouvalides, K., Ekinci, Y. L. 2012. An assessment of the earthquakes of ancient Troy, NW Anatolia, Turkey (pp. 171–200). In E. Sharkov (Ed.), Tectonics – Recent advances (chapter 7, pp. 171–200). Ankara: InTech. ISBN: 978-953-51-0675-3.

Kürçer, A., Yalçın, H., Gülen, L., Kalafat, D. 2015. 8 January 2013 Mw = 5.7 North Aegean Sea earthquake and its seismotectonic significance, Geodinamica Acta, 27, 2-3, 175-188, DOI:10.1080/09853111.2014.957503

Kürçer, A., Özalp, S., Özdemir, E., Uygun Güldoğan, Ç., Duman, T.Y. 2016. Yüzey Kırığı Oluşturmuş Faylar üzerinde aktif tektonik ve paleosismolojik araştırmalar hakkında örnek çalışma: Yenice Gönen Fayı, KB Türkiye. Maden Tetkik ve Arama Genel Müdürlüğü, Doğal Kay. ve Eko. Bült. 21, 1-18.

Kürçer, A., Özaksoy, V., Özalp, S., Uygun Güldoğan, Ç., Özdemir, E., Duman, T.Y. 2017. The Manyas Fault Zone (southern Marmara Region, NW Turkey): active tectonics and paleoseismology. Geodinamica Acta, 29, 1, 42-61, DOI: 10.1080/09853111.2017.1294013.

Le Pichon, X Chamot-Rooke, N., Lallemant,S., Noomen, R., Veis, G. 1995. Geodetic determination of the kinematics of central Greece with respect to Europe implications for eastern Mediterranean tectonics, J. Geophys. Res. 100, 12675-12690.

McKenzie, D.P. 1972. Active tectonics of the Mediterranean region. Geophys. J. R. Astron. Soc. 30 (2), 109–185.

McKenzie, D.P. 1978. Active tectonics of the Alpine Himalayan Belt The Aegean Sea and surrounding regions, Geophys. J. R. Astron. Soc. 55, 217-254.

Meade, B., Hager, B., Reilinger, R. 2002. Estimates of seismic potential in the Marmara region from block models of secular deformation constrained by GPS measurements. Bull. Seismol. Soc. Am. 92 (1), 208–215.

Okay, A. İ. Göncüoğlu, M.C. 2004. The Karakaya Complex: a review of data and concepts. Turkish Journal of Earth Sciences 13, 2, 75-95.

Okay, A. İ., Kaşlılar-Özcan, A., İmren, C., Boztepe-Güney, A., Demirbağ, E., Kuşçu, İ. 2000. Active faults and evolving strike-slip basins in the Marmara Sea, northwest Turkey: A multichannel seismic reflection study. Tectonophysics, 321, 189–218.

Örgülü, G., Aktar, M. 2001. Regional moment tensor inversion for strong aftershocks of the August 17, 1999 İzmit earthquake (Mw= 7.4). Geophys. Res. Lett. 28, 371–74

Özalaybey, S., Ergin, M., Aktar, M., Tapırdamaz, C., Biçmen, F., Yörük, A. 2002. The 1999 ˙Izmit earthquake sequence in Turkey: seismological and tectonic aspects. Bull. Seismol. Soc. Am. 92, 376–86.

Özden, S., Bekler, T., Tutkun, S. Z., Kürçer, A., Ateş, Ö., Bekler, F., Kalafat, D., Gündoğdu, E., Bircan, F., Çınar, S., Çağlayan, Ö., Gürgen, M., İşler, H., Yalçınöz, A. 2008. Biga Yarımadası ve Güney Marmara bölgesinin sismotektoniği. Aktif Tektonik Araştırma Grubu 12. Toplantısı, Bildiri Özleri Kitabı, s. 48-49, Akçakoca, Maden Tetkik ve Arama Genel Müdürlüğü, Türkiye.

Papadopoulos, G.A., Kondopoulou, D.P., Leventakis, G.A., Pavlides, S.B. 1986. Seismotectonics of the Aegean region. Tectonophysics 124, 67–84

Pınar, N. 1953. Preliminary Note on the Earthquake of Yenice Gönen, Turkey, March 18, 1953. Bull. Seismol. Soc. Am., vol. 43, pp. 307–310.

Reilinger, R.E., McClusky, S.C., Oral, M.B., King, R.W., Toksöz, M.N., Barka, A.A., Kinik, I., Lenk, O., Sanli, I. 1997. Global positioning system measurements of present day crustal movements in the Arabian–African–Eurasian plate collision zone. J. Geophys. Res. 102, 9983–9999.

Reilinger, R., McClusky, S., Vernant, P., Lawrence, S., Ergintav, S., Çakmak, R., Özener, H., Kadrov, F., Guliev, I., Stepanyan, R., Nadariya, M., Hahubia, G., Mahmoud, S., Sakr, K., ArRajeh, A., Paradissis, D., Al-Aydrus, A., Prilepin, M., Guseva, T., Evren, E., Dmitrotsa, A., Filikov, S.V., Gomez, F., Al-Ghazzi, R., Karam, G. 2006. GPS constraints on continental deformation in the Africa-Arabia-Eurasia continental collision zone and implications for the dynamics of plate interactions. Journal of Geophysical Research 111, B05411.

Rose, C.B. 1994. The 1993 post-Bronze Age excavations at Troia. Studia Troica 4: 75–104

Rose, C.B. 1996. The 1995 post-Bronze Age research and excavations at Troia. Studia Troica 6, 97–101

Selim, H., Tüysüz, O. 2013. The Bursa–Gönen Depression, NW Turkey: a complex basin developed on the North Anatolian Fault. Geol. Mag. 150 (5), 2013, pp. 801–821.

Selim, H., Tüysüz, O., Karabaş, A., Taş, K.Ö. 2013. Morphotectonic evidence from the southern branch of the North Anatolian Fault (NAF) and basins of the south Marmara sub-region, NW Turkey. Quaternary International, 292, 176-192.

Straub, C.S. 1996. Recent crustal deformation and strain accumulation in the Marmara Sea region, N.W. Anatolia, inferred from GPS measurements. unpub. Ph.D. dissertation, Swiss Federal Institute of Technology at Zurich, p.122, plus appendices.

Straub, C., Kahle, H. 1997. Active crustal deformation in the Marmara Sea region, NW Anatolia, inferred from GPS measurements. Geophys. Res. Lett. 22 (18), 2533–2536.

Şengör, A. M. C. 1979. The North Anatolian transform fault: Its age, offset and tectonic significance. Journal of the Geological Society, 136, 269–282.

Şengör, A.M.C. 1980. Türkiye'nin Neotektoniği'nin Esasları, Türkiye Jeoloji Kurumu Konferans Serisi 2.

Şengör, A. M. C., Barka, A. A. 1992. Evolution of escape-related strike-slip systems: Implications for distribution of collisional orogens. 29th International Geological Congress, Kyoto, Japan, Abstracts, 1, 232.

Şengör, A. M. C., Görür, N., Şaroğlu, F. 1985. Strike-slip faulting and related basin formation in zones of tectonic escape: Turkey as a case study. K. T. Biddle, K.T.,Christie-Blick, N. (Eds.), Strike-slip Deformation, Basin Formation and Sedimentation. SEMP Special Publication 37, 227–264.

Şengör, A. M. C., Tüysüz, O., İmren, C., Sakınç, M., Eyidoğan, H., Görür, N., Rangin, C. 2004. The North Anatolian fault: A new look. Annual Review of Earth and Planetary Sciences, 33, 1–77. doi:10.1146/annure.earth.32.101802.120415

Taymaz, T., Jackson, J., McKenzie, D. P. 1991. Active tectonics of the north and central Aegean Sea. Geophysical Journal International, 106, 433–490.